ENERGY ABSORPTION BEHAVIOUR OF FILAMENT WOUND GLASS AND CARBON EPOXIES COMPOSITE TUBES

by

Auwal MUHAMMAD

June 2014

ENERGY ABSORPTION BEHAVIOUR OF FILAMENT WOUND GLASS AND CARBON EPOXIES COMPOSITE TUBES

by

Auwal MUHAMMAD

A thesis submitted to

the Graduate Institute of Sciences and Engineering

of

Meliksah University

in partial fulfillment of the requirements for the degree of

Master of Science

in

Material Science and Mechanical Engineering

June 2014
Kayseri, Turkey

APPROVAL PAGE

This is to certify that I have read the thesis entitled "Energy absorption behavior of filament wound glass and carbon epoxies composite tubes" by Auwal MUHAMMAD and that in my opinion it is fully adequate, in scope and quality, as a thesis for the degree of Master of Science in Material Science and Mechanical Engineering, the Graduate Institute of Science and Engineering, Melikşah University.

_____

June, 2014 Yrd. Doç. Dr. Ercan Şevkat
Supervisor

I certify that this thesis satisfies all the requirements as a thesis for the degree of Master of Science.

_____

June, 2014 Prof. Dr. M. H. Keleştemur
Head of Department

Examining Committee Members

Yrd. Doç. Ercan Şevhat	June 16, 2014	_____
Prof. Dr. M. H. Keleştemur	June 16, 2014	_____
Yrd. Doç. Dr. Mustafa Yıldırım	June 16, 2014	_____

It is approved that this thesis has been written in compliance with the formatting rules laid down by the Graduate Institute of Science and Engineering.

_____

Prof. Dr. M. Halidun Keleştemur
Director

June, 2014

ABSTRACT

ENERGY ABSORPTION BEHAVIOUR OF FILAMENT WOUND GLASS AND CARBON EPOXIES COMPOSITE TUBES

Auwal MUHAMMAD

M.S. Thesis Material Science and Mechanical Engineering
June 2014

Supervisor: Ass. Prof. Dr. Ercan SEVKAT

ABSTRACT

Compression test on glass and carbon fiber epoxy composites tubes were conducted. Effect of diameter, winding angle, tube thickness and fiber type on the load-displacement behavior as well as energy absorption of composites tubes has been investigated. All these parameters found to be effective on the load-displacement behavior and energy absorption capacity of composite tubes. Results obtained from the study shows that, carbon epoxy stands higher load and energy absorption capability than glass epoxy. To simulate the behavior of composite tubes ABAQUS Finite Element Software package was used. Elastic orthotropic material model along with a Hashin Damage model was employed to simulate the load-displacement relations of carbon and glass composite tubes. FE predicted and experimental load displacement curves matched well up to the first failure of the tubes. The FE predicted and experimentally obtained maximum loads were very close. However the FE predicted behavior after the first failure zone deviated from experimental results. The level of deviation was different for each case. Hence FE predicted and experimental energy absorption was not the same.

Keywords: Energy absorption, carbon fiber, glass fiber, composite tubes, Finite element analysis

ÖZET

Elyaf Sarım Yöntemiyle Üretilen Cam ve Karbon Fiber Epoksi Kompozit Tüplerde Enerji Yutma Davranışı

Auwal MUHAMMAD

Yüksek Lisans Tezi– Malzeme bilimi ve Makine Mühendisliği
Haziran 2014

Tez Yöneticisi: Ass. Prof. Dr. Ercan SEVKAT

ÖZET

Karbon ve cam elyaf takviyeli epoksi kompozit tüpler üzerinde bası deneyleri yapıldı. Çap, sarım açısı, silindirik tüplerin cidar kalınlığı ve elyaf cinsinin kuvvet-deplasman ilişikleri ve enerji yutma kapasitesi üzerindeki etkileri araştırıldı. İncelenen tüm parametrelerin hem kuvvet-deplasman ilişkileri hem de enerji yutma kapasiteleri üzerinde etkili olduğu görüldü. Karbon elyaf takviyeli epoksi kompozit tüplerin cam elyaf takviyeli olanlara göre daha iyi enerji yutma sergilediği tespit edildi. Kompozit tüplerin davranışlarını simule etmek için ABAQUS sonlu elemanlar yazılım paketi kullanıldı. Elastik ortotropik malzeme modeli ve Hashin hasar modeli birlikte tüplerin kuvvet-deplasman ilişkilerini simule etmek için kullanıldı. İlk hasarın meydana gelmesine kadar deneysel ve simülasyon sonuçlarının birbirine çok yakın olduğu fakat hasardan sonra simülasyon sonuçlarının farklılık gösterdiği tespit edildi. Bu farklılık her bir test için farklılık gösterdi. Sonuç olarak simülasyon sonucu elde edilen ve deneysel enerji yutma kapasitelerinde farklılık oluştu.

Anahtar Kelimeler: Enerji yutma, karbon fiber, cam fiber, kompozit tüpler, Sonlu elemanlar yöntemi

DEDICATION

To my parents

ACKNOWLEDGEMENT

I express my sincere appreciation to His Excellency Executive Governor of Kano State for sponsoring me to study Master's in Material science and Mechanical Engineering in Turkey, may Allah reward him abundantly.

I express my sincere gratitude and appreciation to my supervisor Ass. Prof. Dr. Ercan Sevkat for his valuable advice, suggestion, encouragement during this research work. His mutual understanding and good guidance during this work is highly commendable.

My thanks go to the other faculty members for their valuable suggestions and comments. The technical assistance in person of Tuncay is gratefully acknowledged.

I express my thanks and appreciation to management and staffs of physics department, Kano University of science and Technology, wudil, Nigeria for their support and assistance during my stay in Turkey.

I express my thanks and appreciation to my family for their understanding, motivation and patience.

My special thanks to my research mate Abubakar G. Muhammad for his encouragement and valuable suggestion. Lastly, I am thankful to all my colleagues and friends who made my stay at the university a memorable and valuable experience.

TABLE OF CONTENTS

LIST OF TABLES

TABLE

LIST OF FIGURES

FIGURE

CHAPTER 1

GENERAL INTRODUCTION

Understanding energy absorption of materials is especially important for automotive industry due to safety reasons. Commonly used energy absorbers in the automotive industry are manufactured from steel, which are used as bumpers in the front of vehicles. Their aim is to absorb energy in the event of an accident. However, they predominantly fail in a folding manner, a load-displacement behavior similar to that presented in Figure 1.1. The crashworthiness can be significantly improved by the use of composite energy absorbers. Composite have the potential to absorb considerably large amount of energy due to damage modes, including matrix deformation, delamination, local cracking and crushing. Energy absorption capability of a vehicle and success rate of protecting it is occupant is called crashworthiness. Increasing public demand and legislation make crashworthiness an essential requirement in vehicle design and manufacture, from cars and trucks to ships and helicopters. In automotive applications, primary energy absorbers, such as bumpers, are designed to absorb the energy from small impacts seen in circumstances such as parking accidents. Extensive research about energy absorbing properties of composite tubes has shown that, under appropriate conditions and with the correct design, composite materials can offer substantial performance over an equivalent metallic structure. The way they absorb the energy with a constant crush load is in line with the ideal deceleration curve. Metals fail by plastic buckling, which causes oscillations of the crush load. This means that higher deceleration levels are experienced by the occupant for the same level of energy dissipation. Also due to the nature of their failure mode composites are able to crush for greater proportion of their length before the compaction of the material causes the sustained load to rise sharply. Therefore, their importance in the design of modem crashworthy components is growing considerably.

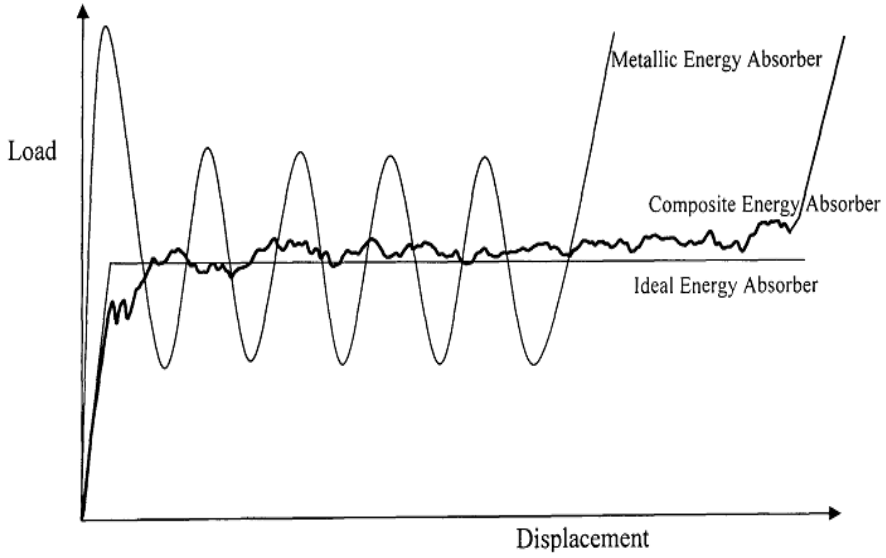

Figure 1.1 Idealized load displacement graph of different energy absorbers

The term composites means material made up of two or more distinct material which combine together but remain uniquely unidentifiable in the mixture. In nature composite materials have been in existence for millions of years, bone, wood, teeth, insect shell and bamboo are just a few examples of the natural occurring composite materials. Man has learned to fabricate composite materials relatively recently. Perhaps, one of the first evidence of a man made composite material is the mud-blocks reinforced with straws. The composite fabrication technology has since progressed from straw reinforced mud-blocks to fiber reinforced polymers, ceramic matrix, metallic matrix and carbon – carbon composite materials [1]. Composite materials are widely used in aircraft and automotive industries. Much attention has been given for over last three decades in studying composite materials. In addition to their excellence performance with high specific strength and stiffness, they also possess good energy absorption behavior. Energy absorption behavior of composite materials is affected by many factors. These factors are geometry and dimension, thickness, fiber orientation angle, fabrication condition.

Manufacturing of composite materials from glass fiber and resin began to appear in 1950s, which is called the “glass steel”. This type of composites is named as glass fiber reinforced

plastics (GFRP). Composite materials can be named by the reinforcement and the matrix materials such as metal matrix composite material, polymer matrix composite material or ceramic matrix composite material. Polymer matrix composites are often named by the type of their reinforced fiber, such as glass fiber composite material which is commonly known as glass fiber reinforced plastics, carbon fiber composite and hybrid fiber composite [2].

1.1 Types of Composite Materials

Composite materials can be categorized using many different criterions: Manufacturing methods, industry that they are manufactured for, and constituent materials. Here composites were categorized by using their constituent materials.

(a) Metal Matrix Composites

Metal matrix composites (MMC) are metals containing of metal alloys reinforced with long fibers, particulates or whiskers. The addition of these reinforcements provides MMCs superior mechanical properties and distinctive physical characteristics. The two most commonly used metal matrices are based on Aluminum and Titanium which both have comparatively low specific gravities. As reinforcement, generally S_iC particles, Boron and Al_2O_3 fibers coated with S_iC are employed due to their ability to provide the needed strength at the lowest weight and least volume [3]. Metal matrix composites are used in a myriad application. The high strength to weight ratio, enhanced mechanical and thermal properties over conventional materials. Increasingly MMCs have been used in several areas including aerospace, transportation (railway and automotive), electronic and thermal management, filamentary superconducting magnets, power conduction, wear resistance and recretational products and sporting goods [4].

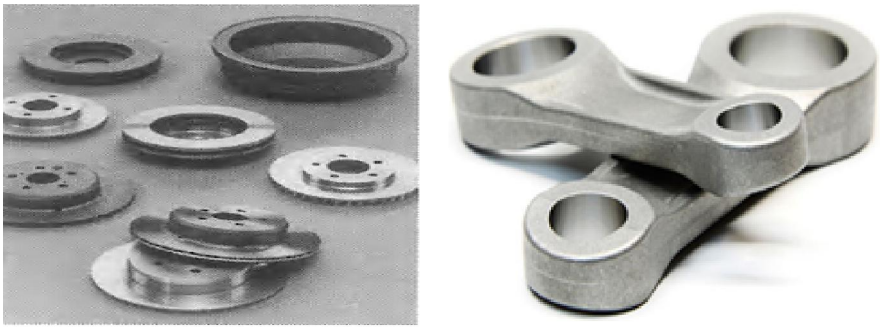

(a) (b)

Figure 1.2 (a) Particulate MMCs for used in brake drums and brake rotors, as a replacement for cast iron (courtesy of D. Miracle) (b) Metal matrix composite rods

(b) Polymer Matrix Composites

The Polymer Matrix Composites consists of polymer such as epoxy, polyester, and Vinyl ester reinforced by bunch of many thin fibers such as graphite, aramids, and boron. For instance graphite/epoxy composites are approximately five times stronger than steel, they are most common composites because of their low cost, high strength, and easy to manufacture. Applications of polymer matrix composites includes military air craft, commercial airlines, space, sporting goods, medical devices, automotive industry, mops with pultruded fiberglass handles and in marine such as boat made of glass fiber [5]. Some examples are presented in figure 1.3.

(a) (b)

Figure 1.3 (a) German fighter plane using glass/epoxy molded fuselage and wing spars of graphite/epoxy (courtesy of Russell A. Lepre) (b) High gain antenna for space

Ceramic Matrix Composites

Ceramic Matrix Composites (CMCs) possess ceramic matrix such as Alumina Calcium, Alumina silicate reinforced by fibers such as carbon or silicon carbide. The most common techniques to manufacture ceramic matrix composites are termed hot processing technique. Ceramic Matrix composite possesses high strength, low density, chemical inertness and service temperature of around 1500℃. CMCs are applicable in high temperature areas whereby metal and polymer matrix composites cannot be used [3]. Carbon/carbon-matrix composites retain much of their strength (up to 2500°C), although they lack oxidation resistance at high temperatures. Fiber materials are usually carbon and aluminum oxide. Applications of CMC include jet and automotive engine components, deep-sea mining equipment, pressure vessels, structural components, cutting tools, and dies for the extrusion and drawing of metals [6]. Figure 1.4 show examples of ceramic matrix composites.

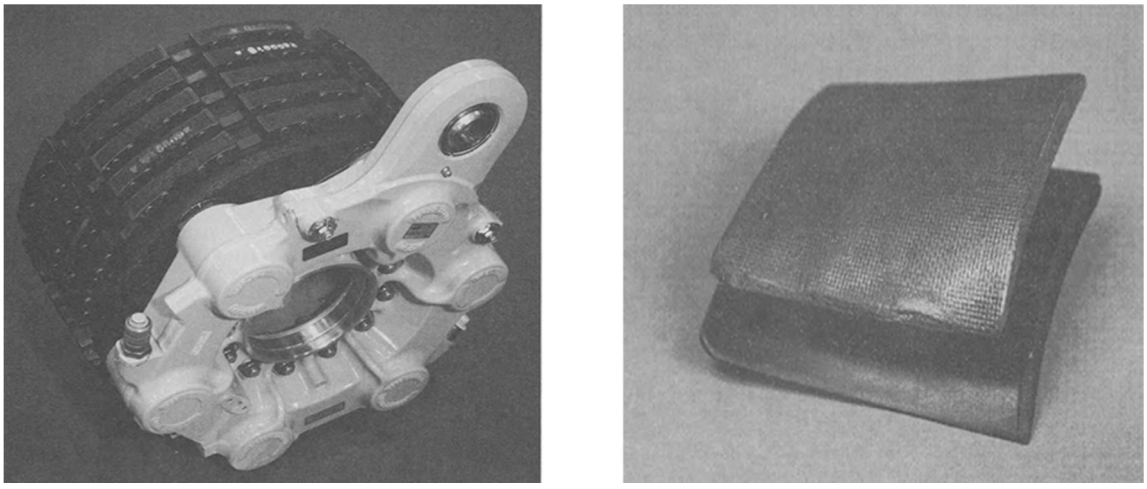

(a) (b)

Figure 1.4 (a) Carbon/carbon brake assembly used on a Boeing 767 plane (Courtesy of Allied Signal Corporation) (b) ceramic matrix composite turbine blades (courtesy of A. R. Hyde)

1.2 Fibers

Fibers consist of thousands of strands; each strand needing a diameter between 5 and 15 micrometers, allowing them to be weaved and braided using textile machines. The bundles

of filaments are known as yarns, tows or roving. These fibers also act as a reinforcement material which gives stiffness, strength and other mechanical properties to the composite materials. Fibers are used in the form of short fibers and long fibers. The short fibers are one with length of few centimeters or fraction of millimeters and mostly used in injection molding while continuous fibers cut through process of manufacturing of composite materials are used as is or woven [7] There are various types of fibers which includes the following:

(a) Fiberglass

Fiberglass is an excellent inorganic nonmetallic material with good performance such as high tensile strength, heat resistance, electric insulation and excellent chemical stability. Glass fiber reinforced plastics have become necessary in most of composite materials industry. Glass fiber is widely used in transportation industries, construction, nuclear power, electronic and electrical appliances, environmental protection, weapons and other traditional industries such as national defense department. It is also used for secondary structure on aircraft, such as fairings, radomes, and wing tips. The blades of helicopter rotor and wind turbines are usually reinforced by glass fiber. There are several types of fiberglass, Electrical glass, or E-glass, is recognized as such for electrical applications. It has high resistance to current flow, S or R glass fiber possesses 20% higher strength than E-glass. They have good retention of high temperature and are only used in situation of high strength, C-glass fiber is a glass fiber with good chemical resistance hence it is suitable for good acid resistance and corrosion resistance, D glass fiber also known as low dielectric glass fiber, they possess good wave penetration properties and is good for reinforcing materials. [2]

(b) Carbon fiber

Carbon fiber is made from carbonization heat treatment of organic fiber such as rayon fiber pitch fiber and it is carbon content is $90\% - 99\%$. Carbon fiber is black in color and is available as dry fabrics. The terms of carbon and graphite fibers are commonly used interchangeable, one of the first differences to be made among carbon and graphite fibers, are based on graphene (hexagonal) layer systems existing in carbon. If the graphene layers, or planes, are stacked with three dimensional order , the material is well-defined as

graphite. Generally extended time and temperature processing is required to form this order, making graphite fibers is more expensive. The bonding between planes is weak [1]. Carbon fibers are very strong and stiffer, 3 to 10 times stiffer than glass fibers. Carbon fiber is more widely used in automobile industry, medical applications, sporting goods. It is also used for structural aircraft applications, such as floor beams, stabilizers, flight controls, and primary fuselage and wing structure. Advantages include its high strength and corrosion resistance. Disadvantages include lower electrical conductivity than aluminum; therefore, a lightning protection mesh or coating is necessary for aircraft parts that are prone to lightning strikes. Another disadvantage of carbon fiber is its high cost.

(c) Aramid fibers

An Aramid fiber offers great potential to produce materials that are lighter in weight, strong, and tough. Aramid fibers also called Kevlar which is DuPont's name for aramid fibers. Two types of Aramid fiber are used in the aviation industry. Kevlar 49 has a high stiffness and Kevlar 29 has a low stiffness. It is currently the most widely used high modulus organic fibers in composite materials. An advantage of aramid fibers is their high resistance to impact damage, so they are often used in areas prone to impact damage, high modulus organic fiber with good corrosion resistance; it is used for military ballistic and body armor applications. The main disadvantage of aramid fibers is their general weakness in compression strength and interlaminar shear strength. Service reports have indicated that some parts made from Kevlar absorb up to 8 percent of their weight in water. Therefore, parts made from aramid fibers need to be protected from the environment. Another disadvantage is that Kevlar is difficult to drill and cut. The fibers fuzz easily and special scissors are needed to cut the material [7].

(d) Boron fibers

Boron fibers are very stiff and have a high tensile and compressive strength. The fibers have a relatively large diameter and do not flex well; consequently, they are available only as a prepreg tape product. An epoxy matrix is often used with the boron fiber. Boron fibers are used to repair cracked aluminum aircraft skins, because the thermal expansion of boron is close to aluminum and there is no galvanic corrosion potentials. Boron fibers are used in military aviation application. Boron fibers are very expansive and can be hazardous.

(e) Ceramic fibers

A ceramic fiber is an alumina silicate based refractory fiber. It is used for high temperature application up to 2300°F. Ceramic fibers are light weight with very low thermal conductivity. They also resist chemical corrosion such as commonly used acids and alkalis [8].

1.3 Matrix materials

During the composite fabrication process matrix materials undergoes a series of the complex process of physical, chemical and physiochemical changes, compound with the reinforced materials to form a whole body with a certain shape. Therefore, the matrix materials directly affect the properties of composite materials. The mechanical properties of composites particularly, the longitudinal tensile properties depend only on the reinforcing material, but the role of a matrix are equally important to consider.

Polymer matrix bonds the reinforcing material into a whole and transfer load among the fibers so that the load is uniformly distributed. The transverse tensile properties, compressive properties, and shear properties are related to matrix [2]. The roles of a matrix in a fiber reinforced composite are, to transfer stresses between the fibers, to keep the fibers in place, and to provide a fence against environmental hazard such as chemicals and moisture. The contact between fibers and matrix is similarly significant in designing damage tolerant structure; hence the processing and weaknesses in composite material depend powerfully on the processing characteristics of matrix. For instance epoxy polymer used as matrix in various aerospace composites, the processing characteristics includes the liquid viscosity, curing temperature and curing time [9].

The most common matrix materials that have been used in commercial and research classified as thermosetting and thermoplastics. Thermoplastics resin is normally used with short fiber reinforced composites.

(a) Thermosetting

Resin is a general term used to define the polymer. The resin, its chemical composition, and physical properties primarily affect the processing, manufacturing, and ultimate properties of a composite material. Thermosetting resins are widely used of all man-made materials. They are easily poured or formed into any shape, are compatible with most other materials,

and cure readily (by heat or catalyst) into an insoluble solid. Thermosetting resins are also excellent adhesives and bonding agents. Thermosetting resin includes epoxies, polyesters, vinyl ester, phenolic resin, polyimides, polybenzimidazoles (PBI), Bismaleimides (BMI), Polyether Ether ketone (PEEK), are more commonly used as matrix material in long fiber reinforced composites, because of their easy processing due to their low viscosity.

Among this thermosetting resin, epoxy is commonly and widely used for fiber matrix composites and is explained here because is used in the present study. Epoxies are the most common matrix material for high-performance composites and adhesives. They have an excellent combination of strength, adhesion, low shrinkage, and processing versatility. Commercial epoxy matrices and adhesives can be as simple as one epoxy and one curing agent; however, most contain a major epoxy, one to three minor epoxies, and one or two curing agents. The minor epoxies are added to provide viscosity control, impart higher elevated temperature properties, and provide lower moisture absorption or to improve toughness [10].

(b) Thermoplastics

Thermoplastic materials are, in general, ductile and tougher than thermoset materials and are used for a wide variety of nonstructural applications without fillers and reinforcements. Thermoplastics can be melted by heating and solidified by cooling, which render them capable of repeated reshaping and reforming. Thermoplastic molecules do not cross-link and therefore they are flexible and reformable. Thermoplastics can be either amorphous or semi-crystalline. In amorphous thermoplastics, molecules are randomly arranged; whereas in the crystalline region of semi-crystalline plastics, molecules are arranged in an orderly fashion [11]. Some of the properties of thermoplastics are given in table 1.1

Table 1.1 Typical thermoplastics resin properties

Resin Material	Density (g/cm^3)	Tensile Modulus GPa (10^6 psi)	Tensile Strength MPa (10^3 psi)
Nylon	1.1	1.3–3.5 (0.2–0.5)	55–90 (8–13)
PEEK	1.3–1.35	3.5–4.4 (0.5–0.6)	100 (14.5)
PPS	1.3–1.4	3.4 (0.49)	80 (11.6)
Polyester	1.3–1.4	2.1–2.8 (0.3–0.4)	55–60 (8–8.7)
Polycarbonate	1.2	2.1–3.5 (0.3–0.5)	55–70 (8–10)
Acetal	1.4	3.5 (0.5)	70 (10)
Polyethylene	0.9–1.0	0.7–1.4 (0.1–0.2)	20–35 (2.9–5)
Teflon	2.1–2.3	—	10–35 (1.5–5.0)

1.4 Manufacturing methods of composite materials

There are various techniques used in fabrication of fiber reinforced polymer composite materials. The most commonly used techniques are:

(a) **Wet lay-up**: It is capable of making very large parts with minimal tooling costs, such as custom built yacht hulls. In the wet lay-up process, a dry reinforcement, usually a woven glass cloth is placed manually on the mold. A low-viscosity liquid resin is then applied to the reinforcement by pouring, brushing, or spraying. Squeegees or rollers are used to densify the lay-up, thoroughly wetting the reinforcement with the resin and removing excess resin and entrapped air [10].

(b) **Vacuum Bag**: A flexible film (e.g., nylon) is placed over the completed lay-up or spray-up, its joints are sealed, and a vacuum is drawn. Bleeders and breathers can be used to remove excess resin and promote the evacuation of air. The vacuum bag pressure helps minimize voids in the laminate and forces excess resin and air from the lay-up. The addition of pressure also yields higher reinforcement concentrations and provides better adhesion between the layers [10].

(c) **Autoclave** : either a vacuum bag or a pressure bag process can be further improved by using an autoclave , which provides additional heat and pressure capabilities, producing greater laminate densification. This process is usually employed in the production of high-performance laminates using epoxy resin systems in aircraft and aerospace applications [10].

(d) **Spray lay – up**: Spray-up processes are very similar to those in the wet lay-up process. In this process, the release agent is first applied to the mold and then a layer of gel coat is applied. The gel coat is left for 2hr, until it hardens. Once the gel coat hardens, a spray gun is used to deposit the fiber resin mixture onto the surface of the mold [11].

(e) **Pultrusion**: Pultrusion is a mature process that has been used in commercial applications since the 1950s. In the pultrusion process, continuous fibrous reinforcement is impregnated with a matrix and is then continuously consolidated into a solid composite. The reinforcement, usually glass rovings, is pulled from

packages on a creel stand and gradually brought together and pulled into an open resin bath where the reinforcement is impregnated with liquid resin [10].

(f) **Resin transfer molding**: The resin transfer molding (RTM) process is also known as a liquid transfer molding process. Although injection molding and compression molding processes have gained popularity as high-volume production methods, their use is mostly limited to nonstructural applications because of the use of molding compounds (short fiber composites). The RTM process is a closed mold operation in which a dry fiber preform is placed inside a mold and then the thermoset resin is injected through an inlet port until the mold is filled with resin. The resin is then cured and the part is removed from the mold [11].

(g) **Filament Winding**: Filament winding is a type of manufacturing procedure, where by controlled amount of resin and oriented fibers are wound around a rotating mandrel and cured to produce the required composite parts, usually in the form of cylindrical structures. Figure (1.2) shows a filament winding process. A fiber roving is pulled from a series of creels and tensioner that control the tension of the fibers into a resin bath that contains epoxy resin. There is blade attached to resin bath which control excess resin by reducing it from the wetted fiber. Once the fiber is thoroughly impregnated and wiped, it is then wound onto the revolving mandrel. The speed of carriage and the winding speed of the mandrel are controlled so as to generate the desired winding angle patterns. Once the appropriate number of layers has been applied, curing is carried out in an oven or at room temperature, after which the mandrel is removed [3].

In general, filament winding techniques has advantages over others techniques, among are as follows [12] [3].

- It is very economical method in lying material down and very past
- It is highly repetitive and precise in fiber placement
- It is reliable technology for making high performance composite parts
- Winding angle of fiber and resin is accurate, repeatable and gives a great quality inner surface.
- There is less cost, due to less labor intensive

- A very large and thick composite can be manufactured
- It can use straight fibers to cover the whole mandrel area which can be good for structural properties of laminates to match the applied load

Figure 1.5: Filament winding process [13]

1.5 Objective of the study

In this study; the energy absorption capability of glass and carbon epoxy composite tubes under static compressive loading was investigated. The results obtained from compression tests were compared and evaluated. The effect of fiber type, wall thickness of tubes, the diameter of tubes, and the winding angle on the energy absorption was reported. The linear-elastics model accompanied by Hashin Damage model was used for simulating energy absorption behavior of glass epoxy and carbon epoxy tubes. The sufficient agreement between experimental and numerical results was achieved.

CHAPTER 2

LITERATURE REVIEW

Energy absorption can be captured by calculating the area under load – displacement curve obtained from compression tests of tubes. Most composite tubes are made from high strength, high stiffness fibers such as glass, carbon and Kevlar, surrounded with thermosetting resins such as polyester and epoxy that hold fibers together. Unlike ductile metals and thermoplastics, the fibers and resins are brittle in nature and they fail by fracture after an initial elastic deformation.

Fracture strain for typical glass fibers is about 1.5–2.0% and for polyester resins it is between 1.5 and 3.5%. Superficially, it may appear that they would thus absorb less energy than conventional metals. Though, they essentially do well when comparison is made in terms of the specific energy absorbed. Figure 2.1 illustrates typical values of the specific energy for some metals and polymer composite materials, namely, carbon fibers in a thermoplastic polyetheretherketone (PEEK) matrix (carbon/PEEK), carbon fibers in epoxy matrix, glass fibers in epoxy matrix, and chopped strand glass fiber mat-reinforced polyester composites [14].

The high value of energy absorption obtained for carbon fibers with polyetheretherketone matrix is 200kJ/kg which is almost twice of that obtained for carbon-epoxy composites. This was due to the high fracture toughness of the PEEK matrix (Ramakrishna and Hamada, 1998), these have been review in the book of Guoxing Lu and Tongxi Yu, 2003.

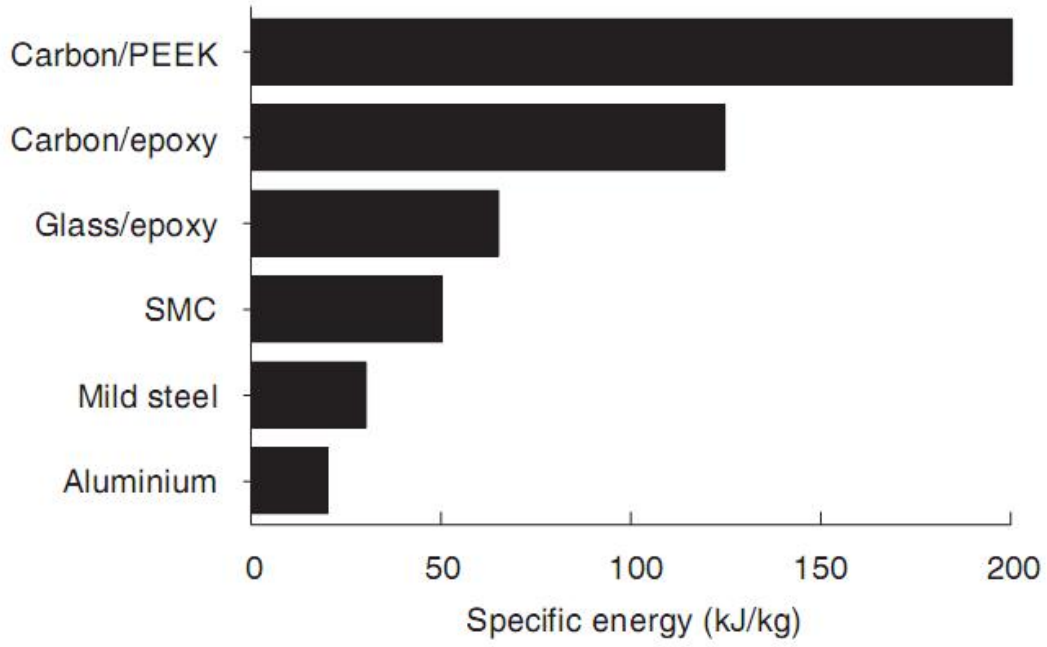

Figure 2.1 Typical values of specific energy absorption for some materials

2.1 Effects of winding angles on energy absorption

The effect of winding angle for filament wound carbon epoxy composite tubes is presented Gang Cheng et.al. [15] Fabricated CFRP tubes using filament winding machine with winding angles of 20°, 40°, 60°and 80 along the axial fiber orientation, were covered with the epoxy resin systems. The result of their studies showed that, the effects of winding angles on compressive strength, strains and compressive modulus of the tubes. With winding angle increasing, the compressive strengths and strains decreased to the minimum value at 40°, and subsequently increased. This compressive failure behavior should be attributed to the overlapping microstructures of the fibers in the tubes with different winding angles. The specific energy absorption, is independent of the structure geometry was used for comparing the energy absorption as indicated in figure 2.2. It was also seen that the highest energy absorption with value of 2.98 kJ/kg at 80° and the lowest with value of 0.49 kJ/kg at 40°, respectively. It was reported that the energy absorption exhibited the similar trend as the strains, which implied that the failure modes of the tubes gradually

transited from ductile failure to brittle failure and then to ductile failure with winding angle as observed in the experiments.

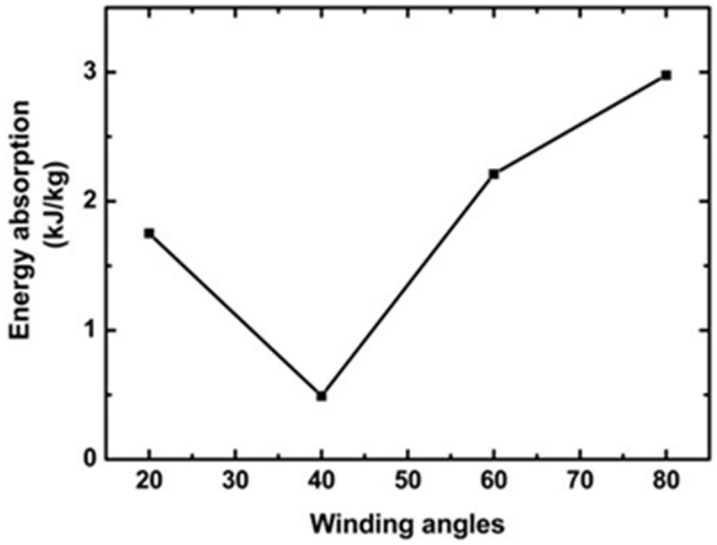

Figure 2.2: Energy absorption with winding angles

Xiaolong Jia et.al. [16] has studied the compression behavior of carbon fiber reinforced polymer tube. Their study revealed that, as winding angle is increase along the longitudinal axis, the compressive strength decrease as indicated in figure 2.3, while the strength value was minimum at winding angle of 40°. The decreasing style was clearly recognized due to the decreasing of load bearing by the fiber and the resultant improvement of longitudinal deformation occur due to the decreasing of fiber alignment along the longitudinal axis with winding angle increasing.

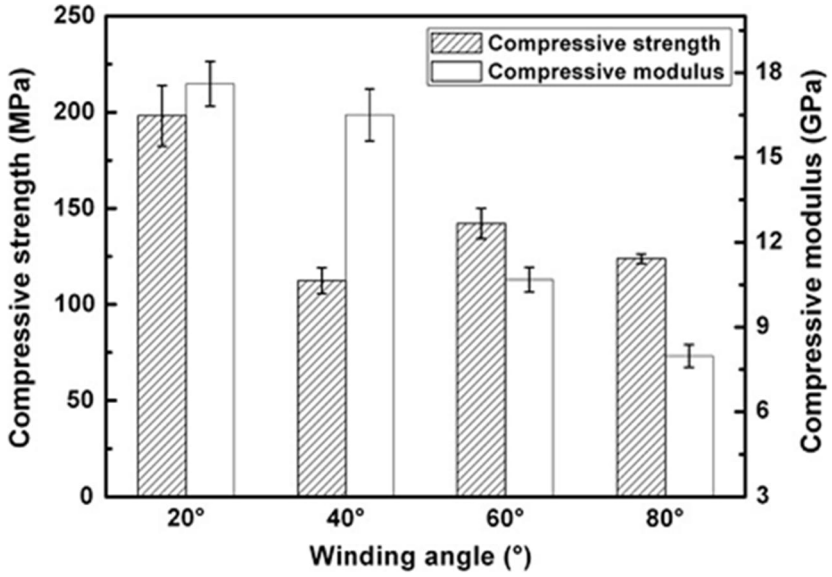

Figure 2.3 (a) Effect of winding angle on compressive strength and modulus of CFRP cylinders (Xiaolong Jia, 2013)

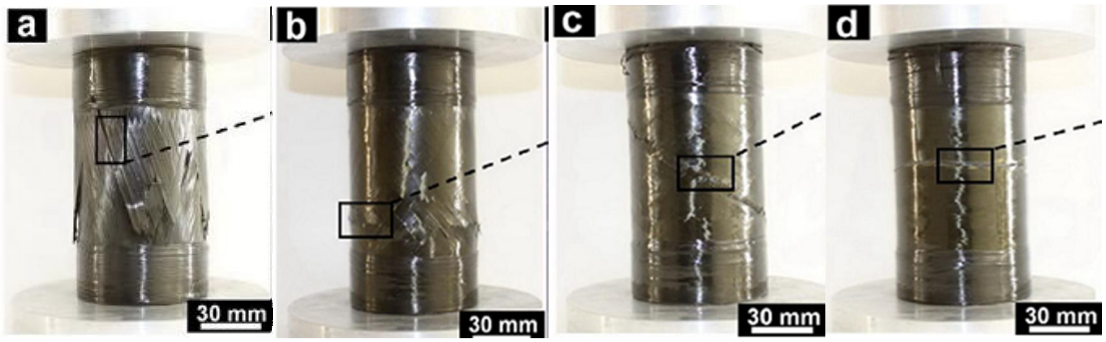

Figure 2.3 (b) Optical images of fractured CFRP cylinders with winding angles of (a) 20° (b) 40° (c) 60° and (d) 80° (Xiaolong Jia, 2013)

It is also noted that in figure 2.3b, the macro-cracks propagated along the direction of winding angles for 20°, 60° and 80°, indicating that the cracks appear perpendicular to the fiber direction. But, in the case of the cylinder with winding angle of 40°, the failure happened along with the plastic deformation in the middle of the specimen and no cracked fibers were witnessed.

2.2. Effects of reinforcing fibers on energy absorption

The types of reinforcing fiber have great effect on energy absorption of composite tubes, Wieslaw Barnat et.al [17] investigated polymer composite material for energy absorbing structures. They reported that, the carbon fiber reinforced epoxy composites absorb 20% more energy than the glass fiber reinforced composites. The largest energy is absorbed by tubes and the smallest is absorbed by the spherical shape. S. H. Lee and Anthony M. Waas [18] investigated the compressive response and fracture characteristics of glass fiber and carbon fiber reinforced unidirectional composite experimentally. The carbon fiber composite was seen to have a lower compressive strength than the glass fiber composites. The conclusion drawn from the studies is that, the carbon fiber composite demonstrated higher stiffness than the glass fiber composite. Stanislaw Ochelski and Pawel Gotowicki [19], in their experimental study, found that the higher energy absorption value is caused by mechanical properties of epoxy reinforced with carbon fibers. It is concluded that the parameters that influence the crushing and bending during the tests are reinforcing fiber, orientation angle of the fiber, fiber content in the composites, number of layers and stacking sequence. The mechanical properties of fibers in the stacking layers and moduli of elasticity have great influence in load – displacement curves. A. S. Abosbaia, et.al [20] in their research finding, they investigated the effect of reinforcing fibers in segmented composite tubes. Figure 2.4, revealed their experimental results. It was indicated that tube made of carbon fiber reinforced polymer has the highest crush failure loads and cotton fabric fiber composite tube showed the stable behavior in comparison with other tested tubes. Tissue mat glass fiber tube possesses the lowest crush failure loads. The stroke efficiency values range is between (79. 7–93.4 %). Furthermore, the highest crushed strain value was attained by cotton fabric fiber tube, whereas tissue mat glass fiber tubes demonstrated the lowest value. Their result indicates unstable load– deformation behavior.

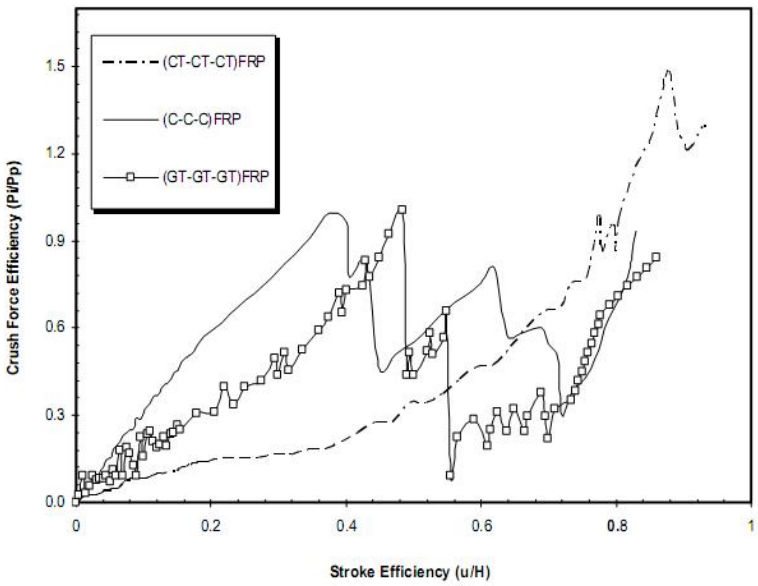

Figure 2.4 Effect of reinforcing fibers on crushing behavior of laterally loaded segmented composite tubes (A. S. Abosbaia, et.al, 2005)

Farley G. L., [21] study the effects of reinforcing fibers on energy absorption of composite materials, the result obtained lead to the conclusion that, the graphite/epoxy composite tubes possess higher specific energy absorption values than that of Kevlar/epoxy and glass/epoxy composite tubes with the same ply orientation. This occurs as a result of lower value of density retain by carbon fibers compared to others used in the study.

2.3. Effects of ply orientation on energy absorption

Gary L. Farley [22] study carbon/epoxy and glass/epoxy tubes specimens with ply orientation of $[0/\pm\theta]_s$ tested under quasi-statistic in order to observe the effect of ply orientations on energy absorption capability. Result obtained showed that, the energy absorption capability of carbon epoxy tube decreases as ply orientation angle θ increases along the axial axis direction, which is similar to the trends of material stiffness or strength as a function of ply orientation. Figure 5, gives graph of energy absorption capability as a function of ply orientation. It's also observed that as θ approaches zero, the highest energy absorption is achieved. As θ increase, the energy absorption capability decreases non-linearly.

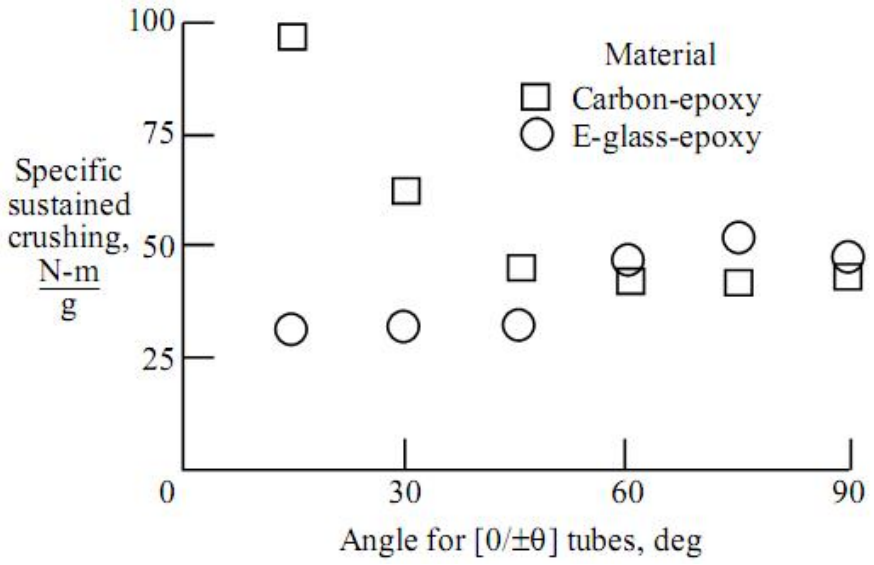

Figure 2.5 Energy absorption capability of $[0/\pm\theta]$ tubes, deg (Gary L. Farley, 1992)

Glass and carbon epoxies tubes have different energy absorption trend as indicated in figure 2.5. When θ is approximately $0°$, the energy absorption of carbon epoxy tube is higher than that of glass epoxy tube. Also the crushing mode observes for glass epoxy tubes is lamina bending, matrix controlled energy absorption response.

Hong-Wei Song et.al, [23] investigated effects of ply orientation on energy absorption of a circular metal tube wrapped with glass epoxy. His results discussed both quasi-static and dynamic test, stating that energy absorption increase as winding angle increase along the transverse direction. The test were carried out with different ply orientation that is$[\pm15°]_3$, $[\pm45°]_3$, and $[\pm90°]_6$ respectively. The metal tube with ply orientation $[\pm15°]_3$ during compression test, give the least energy absorption as the wrapped composite layer doesn't contribute to energy absorption in post buckling stage. Ply with orientation $[\pm45°]_3$, gives moderate energy absorption since its energy dissipation mechanism is mainly composite buckling with least amount of fiber fractured and local delamination, but last ply orientation $[\pm90°]_6$ give a high energy absorption efficiency as a result of breakage of glass/epoxy. Figure 2.6, gives graphical representation of results obtained. The progressive failures observed in both dynamic and static results have similar collapse modes, this is due to low velocity impact in dynamic test which affected by inertia

forces. However, their energy absorption capacities are different. Energy absorption obtained using dynamic test is higher because of the strain rate effect.

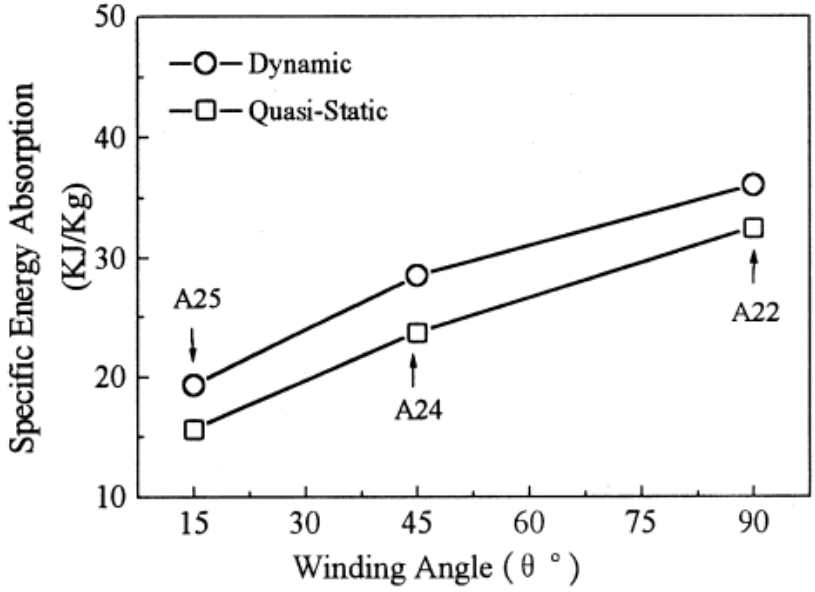

Figure 2.6 Effects of ply orientation on energy absorption

2.4. Effects of specimen geometry on energy absorption

In studying the effect of geometry of the specimen, it can be said that the crush zone fracture mechanisms are influenced by the tube dimensions and these fracture mechanisms determine the overall energy absorption capability of the composite tubes. For a given fiber architecture and geometrical tubes, the specific energy follows the order, of increasing from left to right circular>square> rectangle [24]. Sivakumar Palanivelu et.al [25] studied the energy absorption behavior of glass polyester composite tube with square, circular, and hexagonal cross sectional shapes with thickness of 2mm. The results obtained indicated that, circular tubes stand highest energy absorption and followed by hexagonal and then square tubes. Jose Daniel D. Melo et.al [26] fabricated composite tubes with circular and square cross sectional geometries, and carried out quasi static compression test on the specimens. The results of load – displacement deflection curves behaves linearly up to a maximum load followed by low post failure load which lead to catastrophic failure mode. They also revealed that circular cross-section tubes displayed highest mean crushed stress

in the progressive crushing region when comparing to the other tested specimen. Wieslaw Barnat, et.al [17] Calculated energy absorption of polymer composite with different geometry of the ring section shape, truncate cone shape, wavy coat shape and sphere shape. From the result obtained, the highest energy absorption is seen in the tube with the ring section, followed by the truncate cones, wavy coats, and the lowest is observe by tube with spherical shape. The lowest energy absorption produced by a precise damage mechanism, no fiber cracking, but permanent deformation and bending of the sphere tube occurs during the test.

2.5. Effects of diameters and thickness on energy absorption

Libo Yan, et.al [27] investigated the effect of number of layers for filled and empty flax/epoxy tubes. Their result of finding for all empty tubes indicates that the increase of laminate thickness, will increase the energy absorption, maximum load, and average load values. The highest energy absorption value was obtained in 6-layer laminate tube. Therefore increase in wall thickness is proportional to the increase in total energy and maximum load. The cracks appeared in the tubes during axial crushing test; affect the loading stability and energy absorption behavior. The tubes with diameter of 64 mm and 86 mm with the same thickness were tested. The absorbed energy is higher for the tube with larger diameter and longer displacement crushing can be achieved. Hong-Wei Song [23] investigated the effects of composite thickness on energy absorption of a circular metal tube wrapped with glass epoxy. It was concluded that the property of high strength to weight ratio of composite caused significant increase of crushing load. Their experimental result also indicated that, the energy absorption increase with increasing of wall thickness of composite structure. In the case of specimen type A23, the brittle nature of tubes whose composite layer is thick, limits the external movement of the metal; which may cause unstable catastrophic failure as demonstrated in figure 2.7.

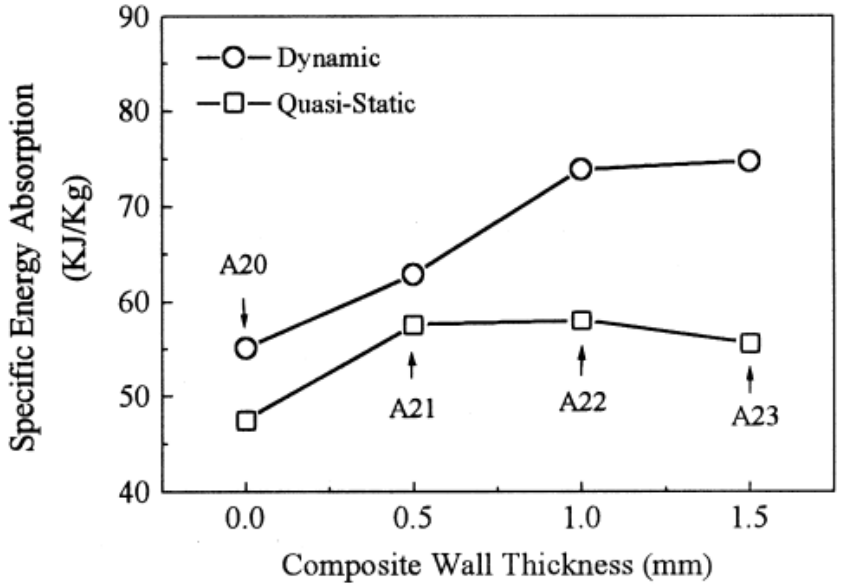

Figure 2.7 Effects of composite wall thickness on energy absorption

Recently, Experimental and numerical methods have been studied by many investigators to analyzed crushing behavior of glass and carbon epoxies composite tube. Some investigated the crushing response subjected to axial compression and compared the results obtained using Abaqus as a numerical tool for simulation and analysis. Ping Zhang et. al [28] the numerical results were in good agreement with quasi static axial crushing tests and also energy absorbing property and failure showed a similar trends with experimental. F. Mustapha and N. W. Sim [29] in their investigation concluded that, there is a good agreement between the experimental and FEA throughout the loading process and also observed that, one percent error is estimated for the peak load between the experiment and failure used to simulate progressive damage. Rizal Zahari [30] he validated the reliability of numerical analysis against results obtained quasi static compression test, which confirms the accuracy of the progressive failure methodology.

There are many experimental studies in the literature which discuss the effect fiber types, matrix types, fiber angle orientation, specimen geometry, diameter and thickness on the energy absorption of composite materials. However, very limited finite element analysis has been done regarding the energy absorption behavior of composite tubes. The present research work used ABAQUS as a numerical tools using progressive damage methodology based on Hashin's failure criterion in order to compared the results with experimental.

CHAPTER 3

MATERIAL AND EXPERIMENTAL PROCEDURE

This chapter will cover the materials used in fabrication of composite tubes; fabrication procedure carried out, cutting the specimens, grinding end of reinforcement and testing procedure will be discussed.

3.1 Specimen Manufacturing

In this study materials required were: E-Glass FWR6-1200 glass fiber and A-38 carbon fiber as reinforcing fibers. Hexion L285 Epoxy and H287 Hardener are used as matrix materials. Peel-ply material between composite and bleeder was used. The removal of excess resin was done using bleeder. Aluminum 6063 tubes with different diameters were used as mandrel. Ren mold-release agent between mandrel and composite was applied before manufacturing. Cylindrical tubes of composite are manufactured using filament winding method. There were twelve composite tubes in total. The size of the tubes has been selected with a length of 1000 mm and diameters of 25 mm, 30 mm and 35 mm respectively. The tubes were manufactured at a two axial computer controlled filament winding machine which required the use of software to generate a machine path. Maximum winding diameter of the machine was 610 mm and the maximum winding length was 4000 mm. The system was capable of utilizing winding angles from 0° to 90° and it's carriages receives a fiber from one creels. The machine can carry a mandrel of maximum 227 kg. The filament winding machine is given in Fig. 3.1**.** Cylindrical tubes of composite are manufacture using filament winding method. Initially ren-release was rubbed on the Aluminum 6063 surface three times at the interval of 20 min, for easy removal of manufactured composite tubes. Then the Aluminum tubes were placed and gripped on the filament winding machine.

Figure 3.1 two axial controlled filament winding machine

Turn on the filament winding machine, once Flexwind completes initialization, the machine's state will be set to emergency stop [E-stop]. Typically, the user will clear this state by clicking the Reset button and then home the machine. Before proceeding, the user should first carry out a visual inspection of the machine to ensure that all axes are clear to move (this need not imply removing any mandrel) [31].

Figure 3.2 Main Flexwind program screenshot.

In loading the machine program, the following procedures were considered

Helical winding was selected as winding pattern. The dialog box was appeared as shown in figure 3.3. The wind parameters were entered correctly and composite designer view all information with the software on the machine. The calculate bottom was pressed to generate fiber path.

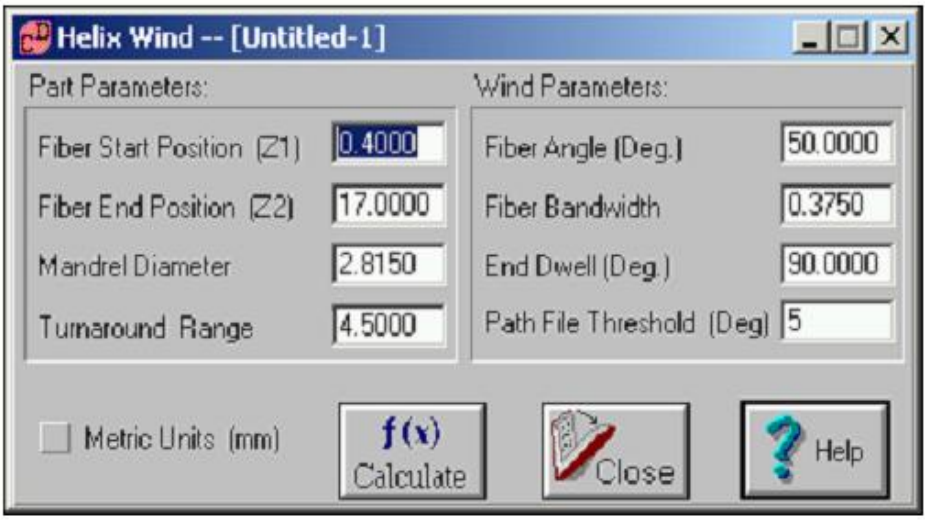

Figure 3.3 Wind pattern selection dialogue box [31]

3.2 Resin system and Reinforcement employed in fabrication

The resin system employed in the fabrication of the tubes is hexion L285 epoxy (100 parts of weight) and H260 S hardener (40 parts of weight). The system is characterized by its good mechanical and dielectric properties and is suitable for filament winding. The properties of these materials are given in table 3.1

Table 3.1 Properties of Hexion L285 and Hardener H 260 S [32]

	Hexion L 285	Hardener H 260 S
Density (g/cm^3)	1.18 – 1.23	0.93 – 0.97
Viscosity [mPas]	600 – 900	80 -100
Amine value [mgKOH/g]	-------	450 - 500
Epoxy equivalent [g/equivalent]	155 – 170	----------
Epoxy value [equivalent/100g]	0.59 – 0.65	----------
Refractory index	1.525 – 1.5300	1.4980 – 1.4985

The reinforcements employed in the fabrication of the tubes are E-glass FWR6-1200 glass fiber and A-38 carbon fiber. The properties are given in table 3.2 and 3.3

Table 3.2 Specifications of glass fiber used [33]

Product name	FWR6
Filament diameter	17
Roving tex count	2400
Type of glass	E
Resin compatibility	Polyester/Vinylester/Epoxy
Moisture content %	Max. 0.15
Coupling agent	Silane

Table 3.3 Carbon fiber properties [34]

	English		Metric		Test Method
Tensile Strength	552	ksi	3800	MPa	ISO 10618
Tensile Modulus	34.8	Msi	240	GPa	ISO 10618
Strain	1.6	%	1.6	%	ISO 10618
Density	0.064	lbs/in³	1.78	g/cm³	ISO 10119
Yield	3,719	ft/lbs	400	g/1000m	ISO 1889
Sizing Type & Amount	D052		1.0 – 1.5	%	ISO 10548
Twist	Never twisted				

3.3 Fabrication of composite test specimens

The tubes were manufactured by using an epoxy resin system with two different fiber types of glass and carbon. For the glass, three different winding angle ($35^{\circ}, 45^{\circ}$ and 55°) and three different mandrel diameters (25 mm, 30 mm and 35 mm) were selecetd. For carbon specimens while the winding angle of 45° was selected, mandrel diameters were same with those used for glass specimens.

The mandrel is supported horizontally between a head and a tail stroke. The tail stroke is driven by required angle and speed using computer program. As the mandrel rotates, a carriage moves along the mandrel and give a fiber with a given position and tension.

Carriage motion is controlled by the computer. Figure 3.4 (a) and (b), represent the process of manufacturing composite tubes using filament winding process.

(a) Glass epoxy (b) Carbon epoxy

Figure 3.4 Manufacturing process of glass epoxy and carbon epoxy composite tubes

Fiber passed through a resin bath and get wet before winding operation. The amount of resin was reduced with a blade which was attached on the resin bath. Once the composite tubes are manufactured, a blanket and Teflon were wrapped on the tubes and tighten it with the plastic tape in order to absorb the excess resin as shown in figure (3.5a).

Manufactured tubes were kept in room temperature for 48 hours and then placed in the furnace which is given in Figure 3.5(b) for curing. Curing operation was carried out at 60℃ for 15 hours.

(a) (b)

Figure 3.5 (a) Teflon, blanket and tape wrapped on the manufactured tubes (b) Curing furnace

Once the tubes are manufactured and cured, they were cut into 50 mm of length by means of laid machine given in Figure 3.6. Three tubes for each specimen types were cut with equal length. During compression test of tubes three tests were conducted for each type in order to get the better result consistency. To have better fit in the test fixtures, the reinforcement region were grinded.

(a) (b)

Figure 3.6 mechanical cutting machines

3.4 Test procedures

Computer controlled Instron-43 Universal testing machine was used for compression test with a load capacity of 50 KN. The test rate was adjusted to 0.1 mm/s. The tests were conducted in room temperature and break threshold was also adjusted depending with the thickness and diameter of the tubes. Composite tubes were compressed between two parallel grips. While the upper grip was moving the lower one was stationary. The fixed grip was fitted with a load cell from which the load signal, crosshead displacement and time were stored in the computer. In each test the load was assigned as the Y-axis and the crosshead displacement as X-axis. For all composites compression tests, progressive crushing occurred. Figure 3.7 gives MTS Instron-43 Computer-controlled machine

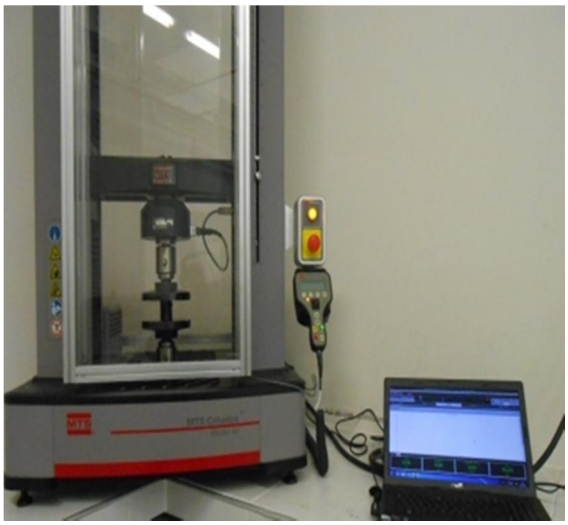

Figure 3.7 MTS Instron-43 Computer-controlled machine

CHAPTER 4

RESULTS AND DISCUSSIONS

Compression tests were carried out on each cylindrical composite tube. -The load-displacement response and energy absorption capability of cylindrical composite tubes were recorded and calculated respectively. The effects of using different fibers, winding angles, thickness and diameters were studied. The energy absorbed during progressive crushing of composite tube is the area under load-displacement curve. Energy absorption of glass/epoxy and carbon/epoxy of composite tubes were calculated from load-displacement curves with graphical method.

4.1 Effects of thickness on energy absorption capability of glass and carbon epoxies composite tubes

The load-displacement curves of glass and carbon epoxy composite tubes obtained from compression tests were presented in Figure 4.1 a & b respectively. The specimens with one, two and three layers with 50 mm length and 35 mm diameter were considered. The load-displacement curves behaves linearly first and then specimen cracked since the absorbed energy exceeds the threshold of material properties at the crush zone due to the crack, instant drop in the load was observed. Initial load for 1 layer glass/epoxy specimen was 2.01 KN, and then load dropped to 0.66 KN, and increased to 0.94 KN at the end of 32 mm axial displacement. For 2 layer glass/epoxy, maximum load was 7.94 KN, then the load dropped to 1.91 KN, and then increased to 4.39 KN at the end of 32 mm axial displacement. The maximum load for 3 layer glass/epoxy was obtained as 12.01 KN, then load dropped to 2.60 KN, and then increased to 5.21 KN at the end of 33 mm of axial displacement. During the static test of glass epoxy composite tube, damage was observed as white line forming along the fiber/matrix. The crack formation in the matrix and

fiber/matrix debonding was presented in Figure 4.2(a). This is consistent with the observation made in [35]

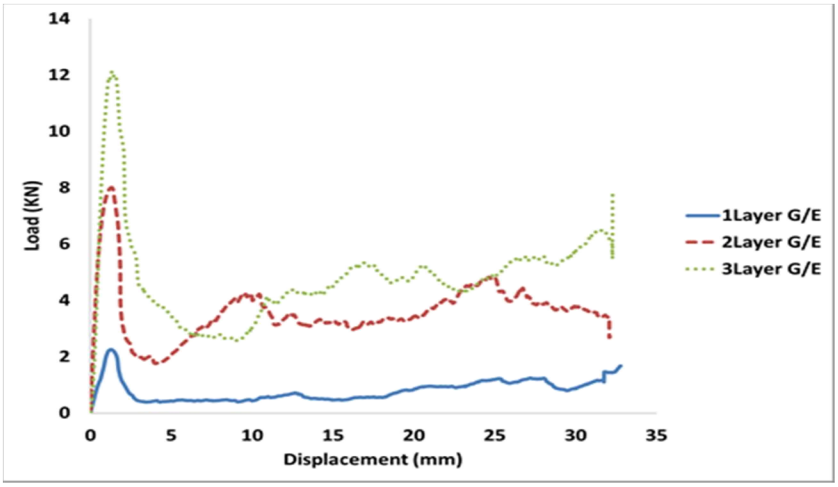

(a) Load – Displacement curves for Glass/epoxy

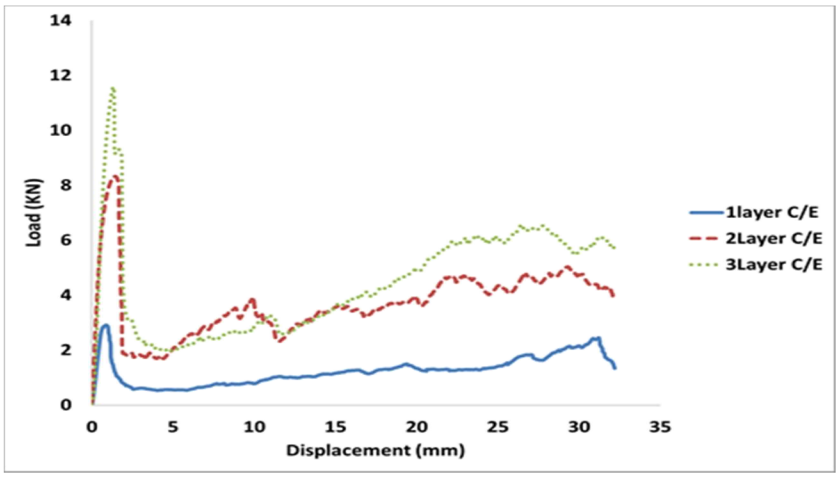

(b) Load – Displacement curve for Carbon/epoxy

Figure 4.1 Graph of Load – Displacement curve for glass epoxy and carbon epoxy with 35 mm diameter

Pictures of crushed glass epoxy and carbon epoxy tubes snapped at interval of 5 mm displacement are presented in Figure 4.2(a) and (b)

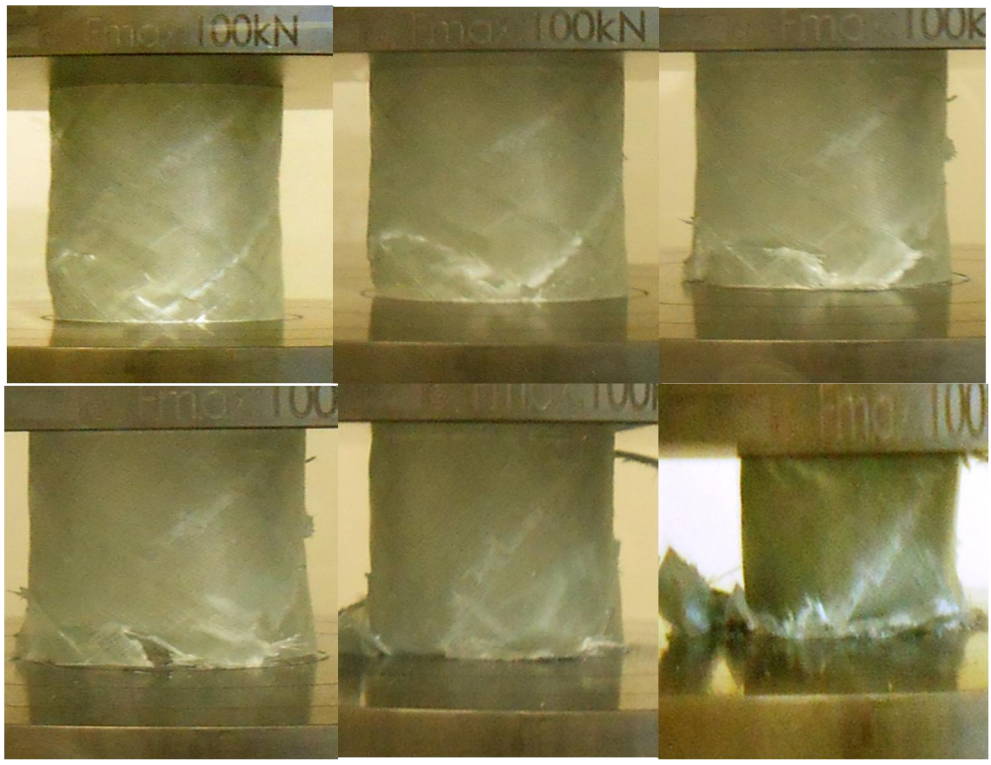

Figure4.2 (a): Crushing sequence of a glass epoxy composite tubes

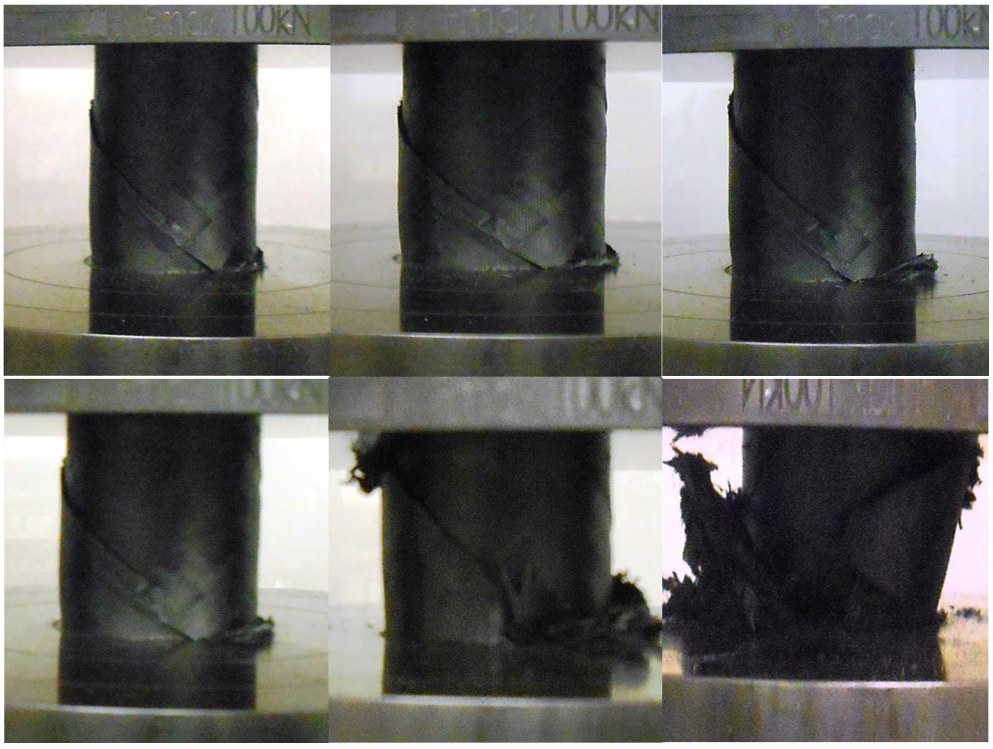

Figure 4.2 (b) Crushing sequence of a carbon epoxy composite tubes

In the case of carbon/epoxy, maximum load for 1 layer was 2.65 KN then dropped to 0.75 KN and then increased to 0.95 KN at the end of 33 mm axial displacementload. For 2 layer maximum load was 8.34 KN, then the load dropped to 2.11 KN, and then increased to 4.63 KN at the end of 32 mm axial displacement. The maximum load for 3 layer carbon/epoxy was obtained as 11.37 KN, then load dropped to 2.02 KN, and then increased to 6.42 KN and then dropped to 5.21 KN at the end of 33 mm of axial displacement. During the compression test, crack noise failure could be heard in the initial stages of the experiment, this noise arose as damage mechanism which attributed to delamination and fiber fracture. Figure 4.2 (b) shows the growth and accumulation of damage within the composite tubes. However it was observed during the experiment that, after initial crack, progressive damage initiated at the bottom and collapse more significantly at the bottom of the tubes.

Figure 4.3 (a) and (b) represent the final crushed shape of carbon/epoxy and glass/epoxy respectively. When the tubes is compressed, the material start shearing off at the edge of tubes, as the loading progress the shearing fractured become more obvious. Both the tubes shatter at the bottom and collapse more significant at the bottom of the tube.

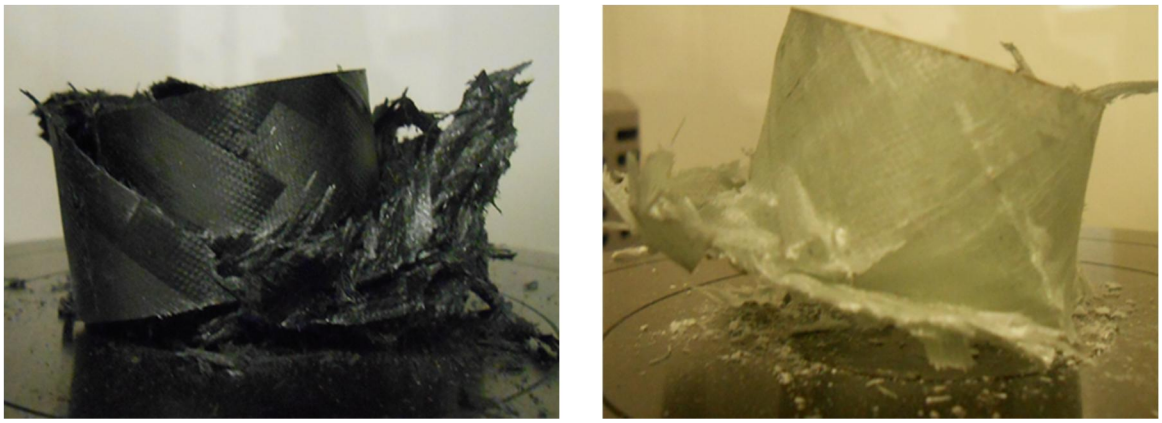

(a) Final crushed shape of carbon/epoxy (b) Final crushed shape of glass/epoxy

Figure 4.3 Final crushed shape glass and carbon epoxies

Table 4.1 showed summary of energy absorption for glass/epoxy and carbon/epoxy composite tubes. It is clearly indicates that, the energy absorption of glass/epoxy and

carbon/epoxy composite tubes were directly affected by the number of layers. Consequently, composite tubes with higher number of layer give greater value of average crushing load which indicated greater value of energy absorption. The energy absorption for 1 layer, 2 layer and 3 layer glass/epoxy and carbon/epoxy were (26.60 KN and 43.70 KN), (115.6 KN and 132.3 KN) and (155.1 KN and 159.2 KN) respectively. It is also observe that composite reinforced with carbon fibers stands much energy absorption as presented in Figure 4.4.

Table 4.1 Energy absorption for glass and carbon epoxies

Number of Layers	Energy absorption (KN-mm)	
	Glass/epoxy	Carbon/epoxy
1 Layer	26.60	43.70
2 Layer	115.6	132.3
3 Layer	155.1	159.2

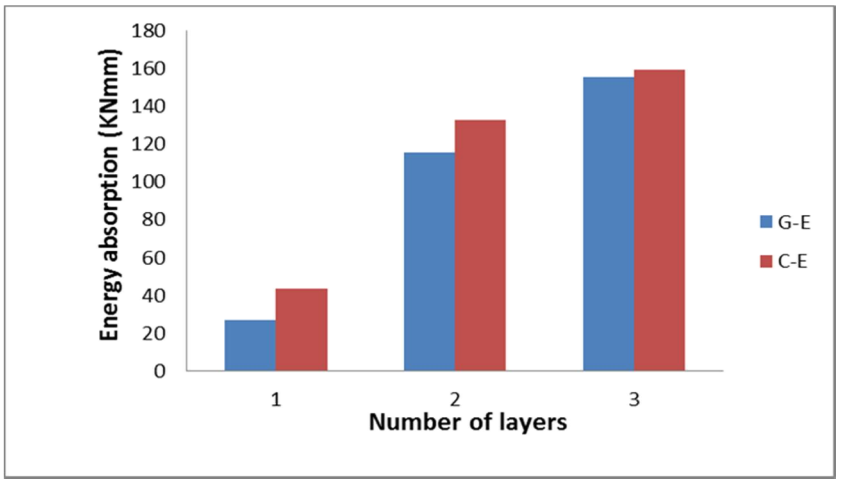

Figure 4.4 Total absorbed crash energy of glass/epoxy and carbon/epoxy with different number of layers

4.2 Effects of diameters on energy absorption capability for glass epoxy composite tubes

Figure 4.5 is a combined diagrams of load-displacement curves of glass/epoxy composite tube with different diameters. It was observed that, the wavelike motion remain constant after initial crush up to failure for 25 mm and 35 mm respectively. But in case of 30 mm diameter, it is good to mention that, the tube demonstrate two different peak load. As the load reached the first maximum peak load it droped to initial position and then the second peak load raised above the first peak load value. This failure observed in the test was undesirable failure (not found in any reviews). It is also noted that, the initial sharp drop in the load for 30 mm of diameter touched the initial and pick up progressively. This could be because of non-parallel cutting of top and bottom of composite tubes. It was observed that, maximum load for 25 mm specimen was 6.75 KN and then load dropped to 1.37 KN and then increased to 3.67 KN at the end of 35 mm axial dispalement. For 30 mm specimen, the maximum load was 7.0 KN and then load dropped to 0.003 KN and pick up progressively. The maximum load for 35 mm diameter was recorded as 8.23 KN then dropped to 0.90 KN and increased to 3.27 KN at the end of 35 mm axial displacement.

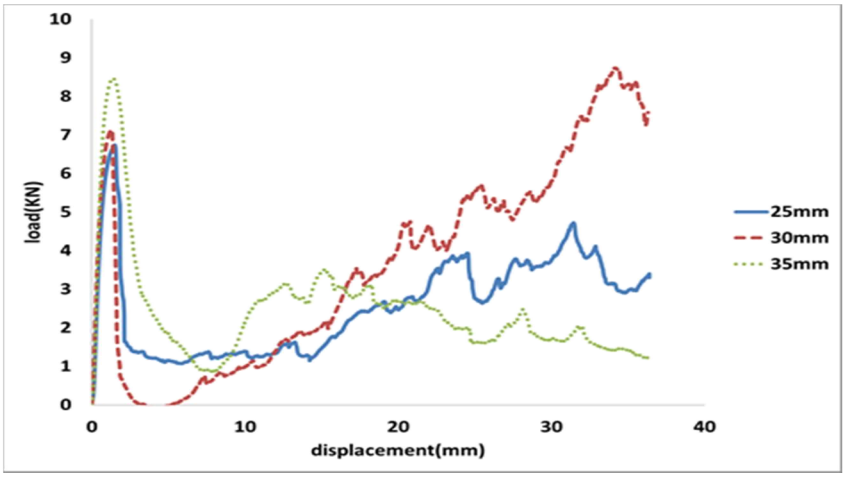

Figure 4.5 Typical crush load –displacement curves with different diameters for glass/epoxy.

Figure 4.6 shows compare the energy absorption capability of glass/epoxy composite tube with different diameters. It was observed that the larger the diameter of the geometry, the

more energy the specimen absorbs. The summary of energy absorption for glass epoxy with different diameter is presented in table 4.2.

Table 4.2 Energy absorption of glass epoxy with different diameters

Different Diameter (mm)	Energy absorption (KN – mm)
25	89.80
30	116.1
35	143.8

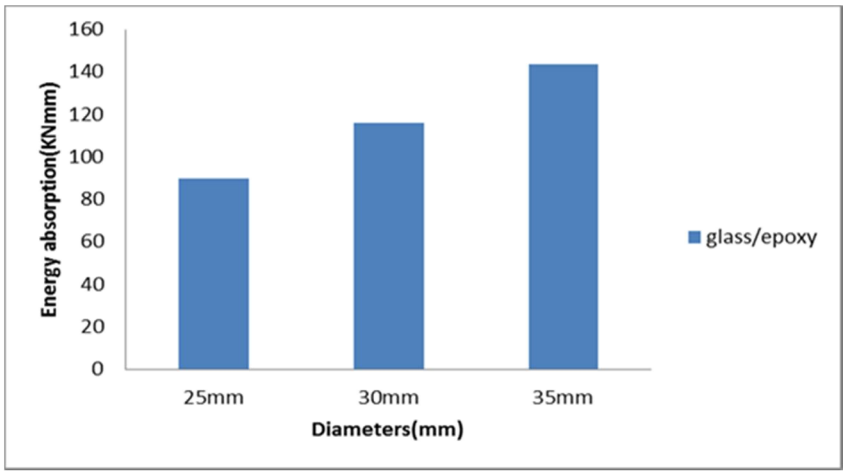

Figure 4.6 Total absorbed crash energy of glass/epoxy with different diameters.

4.3 Effects of winding angles on energy absorption capability of glass epoxy composite tubes

All tubes were fabricated by mandrel wrapping of the fabric pre- impregnated with resin, which was positioned to produce different tubes with fiber orientation. The tubes were wound with two [±35°], [± 45°] and [± 55°] layers with respect to the longitudinal axis of the tubes. Figure 4.7 (a) – (c) gives schematic representation of the angles.

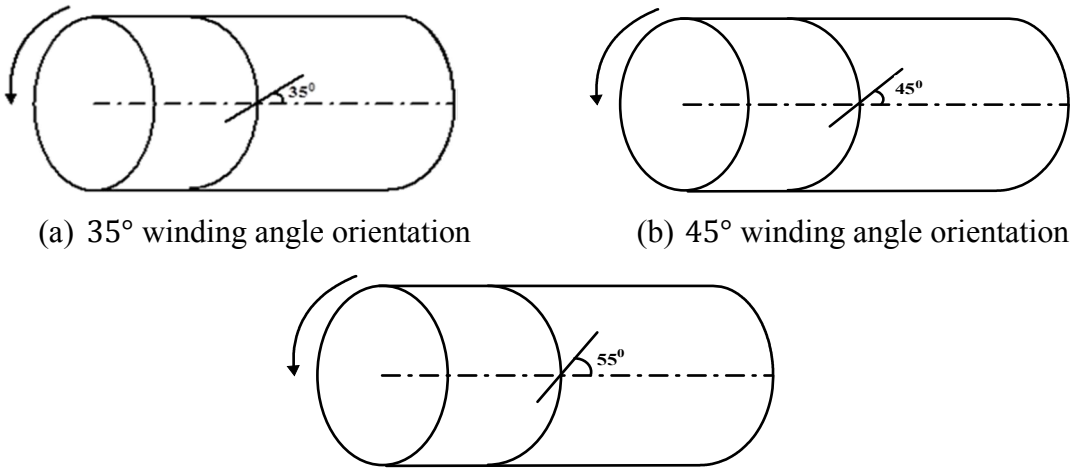

(a) 35° winding angle orientation (b) 45° winding angle orientation

(c) 55° winding angle orientation

Figure 4.7 Different winding angle orientations

Figure 4.8, is a combined diagram of load displacement curves for glass epoxy composite tube with different winding angle. It was clearly observed that for composite tubes under axial compression, the average load fluctuation remain constant after initial crush up to failure for angles 35° and 45° respectively. But in case of angle 55°, two characteristics failure were observe in the test in which the first failure was desired progressive crushing, while the second was undesirable failure, but its effect is somewhere within the damage, before which the tubes crushes progressively. It is clearly seen that, 35 degree accepts higher area than other tested types. Maximum load for 35° specimen was 5.93 KN and then load dropped to 1.21 KN and then increased to 3.65 KN at the end of 33 mm axial dispalement. For 45° specimen, the maximum load was 5.50 KN and then load dropped to 0.55 KN and pick up progressively. The maximum load for 55° specimen was recorded as 5.97 KN then dropped to 0.145 KN and increased to 0.95 KN and then dropped to 0.26 KN and increased to 3.93 KN at the end of 33 mm axial displacement.

Figure 4.8 shows energy absorption capability of glass/epoxy composite tube with different angles. It is clearly seen that, angle 35° stands much energy absorption than the others, this is due to the higher value of average crushing load observed in load-displacement curves. Table (4.3) also presented the value of energy absorption obtained. The energy absorption obtained for 35°, 45°, and 55° were recorded as 86.27 KNmm, 63.07 KNmm and 36.74 KNmm respectively.

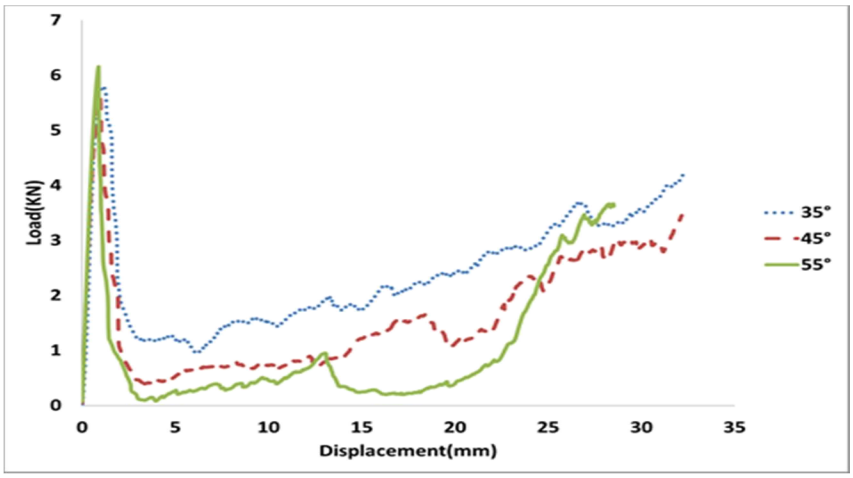

Figure 4.8 Graph of load against displacement of glass epoxy with three different angles.

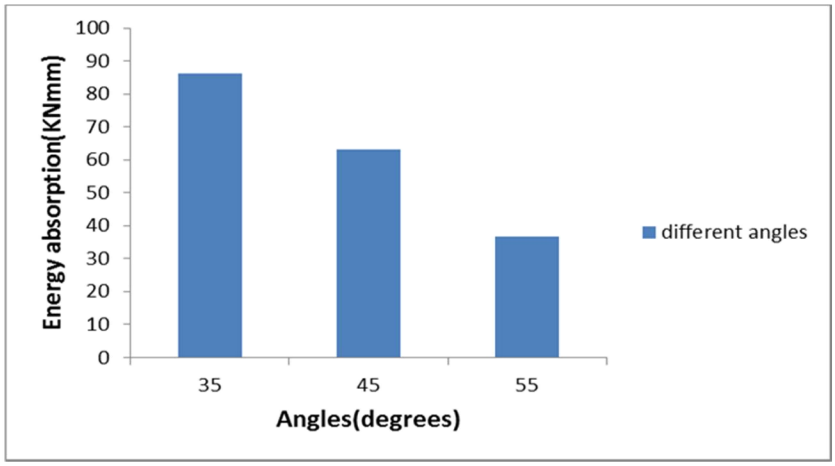

Figure 4.9 Absorbed energy of glass/epoxy and carbon/epoxy with different angles.

Table 4.3: Energy absorption of glass epoxy with different winding angles

Different winding angles (Degrees)	Energy absorption (KN – mm)
35	86.27
45	63.07
55	36.74

CHAPTER 5

FINITE ELEMENT ANALYSIS

The 3-D finite element analyses of compression behavior of composite tubes were modeled using Abaqus, a commercial finite element modeling (FEM) software. The numerical analysis was performed by considering the experimental test parameters.

The computer models developed for this study consisted of multiple unidirectional fiber lamina stacked in various orientations. The element chosen was S4R, 4 nodes doubly curve thin or thick shell, with reduced integration, hourglass control, and finite membrane strains.

A part was created with radius of 17.5 mm and length of 50 mm, thickness of the tube was 1 mm. The dimension and geometry of the specimen was given in figure 5.1.

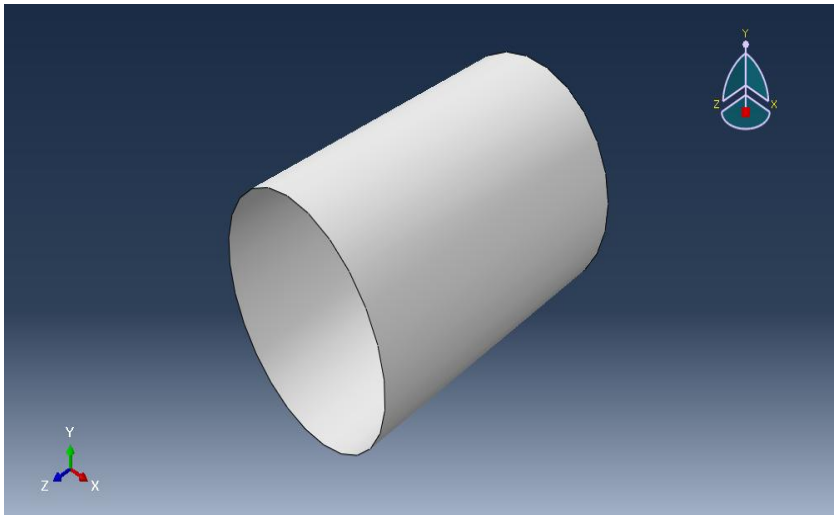

Figure 5.1 Geometry and dimension of the composite tube

The material properties of the composites were obtained from previous research study conducted by our research team [36]. During finite element modeling; strength values

obtained from previous research were reduced match experimental results. This could be due to the fact that strength values of flat tensile specimens reported in previous study does not well represent the strength values of filament wound composite tubes. However elastic constants were the same. The geometric irregularities observed on the surface of the tubes may result in strength reduction. The elastic constants and strength values of glass and carbon epoxy composites were summarized in Table 5.1 and 5.2.

Table 5.1 Glass epoxy material properties

E_1	Young's modulus along fiber direction 1 (MPa)	21040
E_2	Young's modulus along fiber direction 2 (MPa)	6680
γ_{12}	Poisson's ratio	0.33
G_{12}	Shear modulus in 1 – 2 plane (MPa)	900
G_{13}	Shear modulus in 1 – 3 plane (MPa)	850
G_{23}	Shear modulus in 2 – 3 plane (MPa)	850
α	Coefficient that determine contribution of shear stress to the fiber tensile initiation criterion	0.1
X^T	Longitudinal tensile failure stress in fiber direction (direction 1) (MPa)	800
X^C	Longitudinal compressive failure stress in fiber direction (direction 1) (MPa)	358
Y^T	Transverse tensile failure stress in direction 2 (transverse to fiber) (MPa)	125
Y^C	Transverse compressive failure stress in direction 2 (transverse to fiber) (MPa)	90
S^L	Longitudinal shear strength	38
S^T	Compressive shear strength	65

Table 5.2 Carbon epoxy material properties

E_1	Young's modulus along fiber direction 1 (MPa)	34770
E_2	Young's modulus along fiber direction 2 (MPa)	6680
γ_{12}	Poisson's ratio	0.33
G_{12}	Shear modulus in 1 – 2 plane (MPa)	850
G_{13}	Shear modulus in 1 – 3 plane (MPa)	800
G_{23}	Shear modulus in 2 – 3 plane (MPa)	800
α	Coefficient that determine contribution of shear stress to the fiber tensile initiation criterion	0.1
X^T	Longitudinal tensile failure stress in fiber direction (direction 1) (MPa)	900
X^C	Longitudinal compressive failure stress in fiber direction (direction 1) (MPa)	450
Y^T	Transverse tensile failure stress in direction 2 (transverse to fiber) (MPa)	120
Y^C	Transverse compressive failure stress in direction 2 (transverse to fiber) (MPa)	70
S^L	Longitudinal shear strength	33
S^T	Compressive shear strength	60

The composite tube was meshed with approximate global size of 2.5 mm, element deletion turned on and maximum degradation was selected as 0.99.

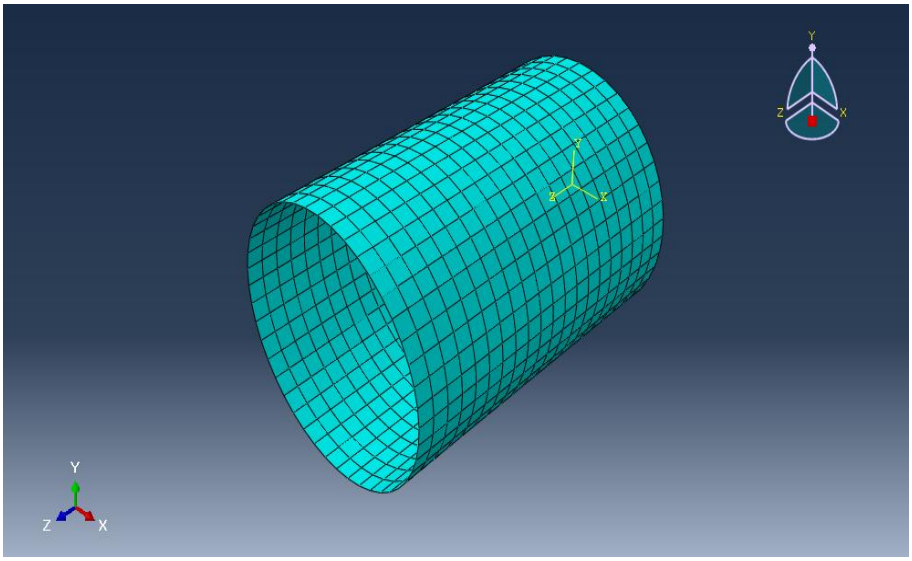

Figure 5.2 Mesh and geometry of glass epoxy tube.

The composite tube was axially compressed between two rigid platens during compression test. So, in the case of modeling, the bottom edge of the tube is fixed and displacement of 35 mm on the upper part of the tube is applied in U3 or Z – direction as shown.

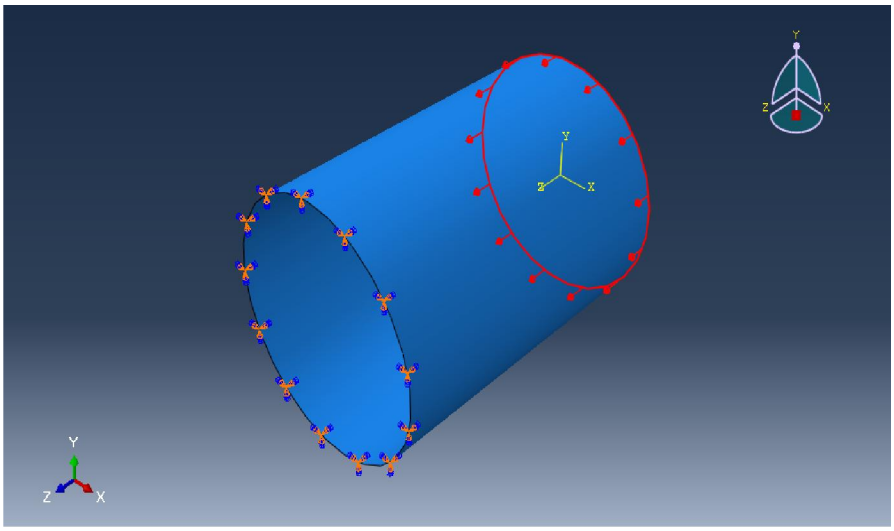

Figure 5.3 Boundary conditions applied to glass epoxy.

The applied displacement causes the cylindrical tube to deform. The deformed shape is shown in figure 12.

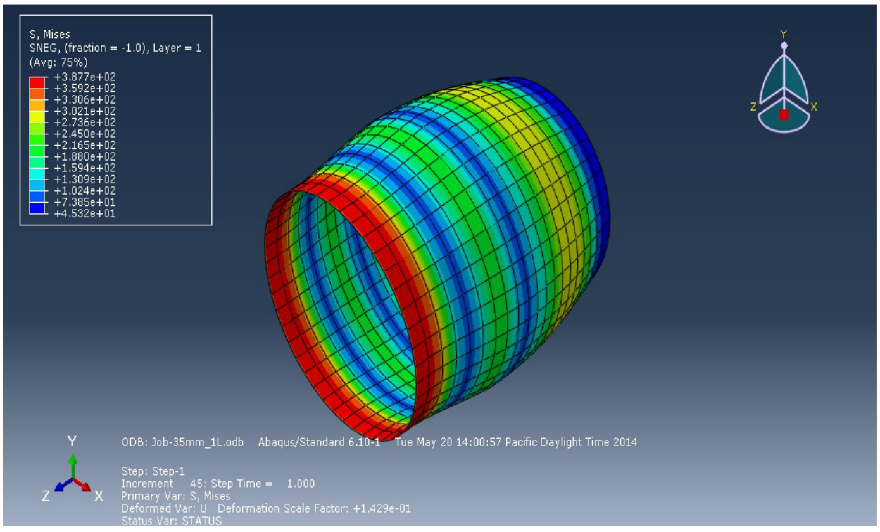

Figure 5.4 Deformed shape of composite tube.

Twelve finite element models with different reinforcement, thickness, diameter and winding angles were created and used in simulations

5.1 Damage and failure

The procedures for predicting the growth of the damage path are developed using the progressive failure analysis methodology implemented within the Abaqus/standard static finite analysis code-[37]. The Hashin damage criterion has been used in this study to predict intra-lamina damage modes such as fiber failures and matrix failures. The intra-lamina failures mode considered were

- Fiber failure in tension and compression,
- Matrix cracking in tension and compression

The Hashin failure criteria are quadratic in nature due to curve fitting not physical reasoning of material behavior [38]. To account for the observed phenomenon of the multi-mode failure of fiber reinforced composites, Hashin introduced four damage initiation criteria for fiber and matrix, tension and compression. The input data for Hashin criteria are the longitudinal tensile and compressive strengths, the transverse tensile and compressive strengths, and the longitudinal and transverse shear strengths. All the strength values are assumed to be positive [39]

The initiation criteria have the following general forms.

Fiber tension ($\hat{\sigma}_{11} \geq 0$):

$$F^t = \left(\frac{\hat{\sigma}_{11}}{X^T}\right)^2 + \alpha\left(\frac{\hat{\gamma}_{12}}{S^L}\right)^2 \quad \text{---------- 4.1}$$

Fiber compression ($\hat{\sigma}_{11} < 0$)

$$F^c = \left(\frac{\hat{\sigma}_{11}}{X^C}\right)^2 \quad \text{---------- 4.2}$$

Matrix tension $\hat{\sigma}_{22} \geq 0$)

$$M^t = \left(\frac{\hat{\sigma}_{22}}{Y^T}\right)^2 + \left(\frac{\hat{\gamma}_{12}}{S^L}\right)^2 \quad \text{---------- 4.3}$$

Matrix compression ($\hat{\sigma}_{22} < 0$)

$$M^c = \left(\frac{\hat{\sigma}_{22}}{2S^T}\right)^2 + \left[\left(\frac{Y^C}{2S^T}\right)^2 - 1\right]\frac{\hat{\sigma}_{22}}{Y^C} + \left(\frac{\hat{\gamma}_{12}}{S^L}\right)^2 \quad \text{---------- 4.4}$$

Where

X^T : Longitudinal tensile strength

X^C : Longitudinal compressive strength

Y^T: Transverse tensile strength

Y^C: Transverse compressive strength

S^L : Longitudinal shear strength

S^T: Transverse shear strength

α is the coefficient that determine contribution of shear stress to the fiber tensile initiation criterion

$\hat{\sigma}_{11}$, $\hat{\sigma}_{22}$, $\hat{\gamma}_{12}$ are components of the effective tensor $\hat{\sigma}$ that is used to evaluate initiation criteria.

The material properties are degraded based upon the damage mode. In the current work, the fiber failure damage mode is assigned to the DELETE parameter. Hence the damage path prediction is achieved by deleting (or eroding) an element when all of the material points within the element have failed in the fiber failure mode. The maximum degradation used was 0.99. The output variable STATUS will indicate if an element is active or not. A value of 1.0 for the STATUS output variable indicates an active element, and a value of zero indicates a deactivated or deleted element.

5.2. FE simulated energy absorption capability of glass and carbon epoxies tubes with different thickness

FEA results of glass epoxy and carbon epoxy obtained using Abaqus/Standard for the deformation modes and load displacement curve are shown in Figure 5.5 and 5.6 respectively. It is clearly seen that in figure 5.5, at the beginning of the loading operation, the applied load rises linearly up to a maximum load is obtained. The maximum load for 1

layer, 2 layers, and 3 layers glass epoxy were recorded as 2.11 KN, 7.95 KN and 11.99 KN respectively. In case of carbon epoxy, maximum recorded load were observe as 2.70 KN, 7.98 KN and 10.50 KN for different thickness as presented in Figure 5.6.

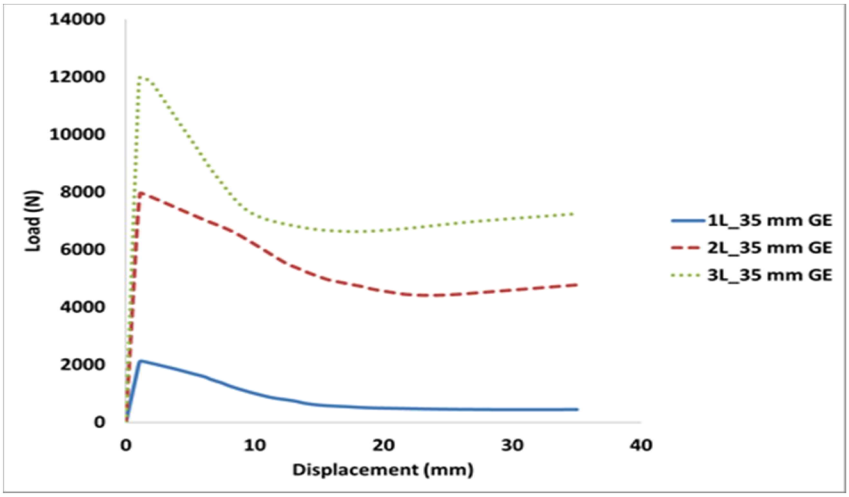

Figure 5.5 Load – Displacement curves for glass epoxy with different thickness.

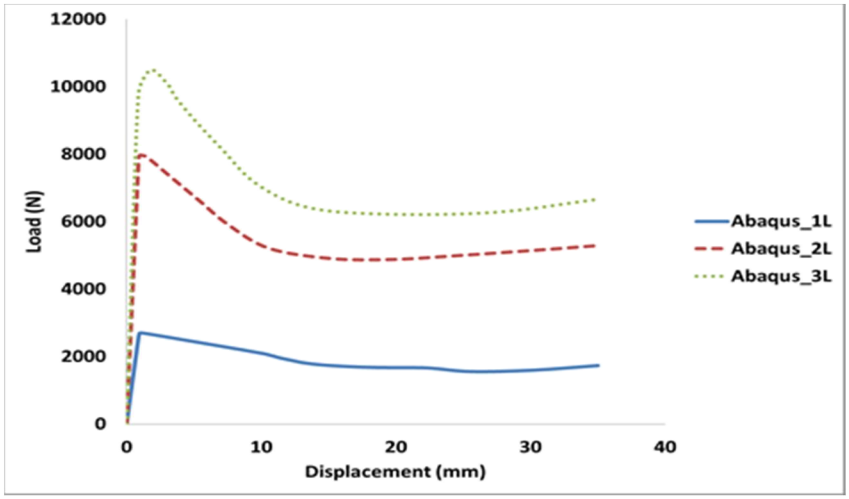

Figure 5.6 Load – Displacement curves for carbon epoxy with different thickness

In all cases, the loads drops off suddenly and move progressively in constant manner.

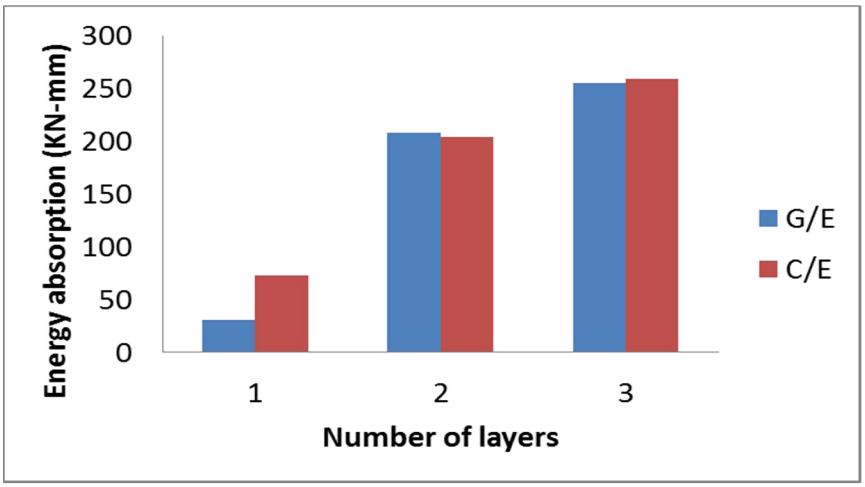

Figure 5.7 Comparison of FE simulated energy absorption capability of glass epoxy and carbon epoxy with different thickness

5.3. FE simulated energy absorption capability of glass epoxy tubes with different diameters

Figure 5.8, is a combined diagrams of load-displacement curves for glass/epoxy composite tube with different diameters obtained using Abaqus/standard. It can be seen that, the applied load at the start of loading process increases linearly up to the point were maximum load is reached. For 25 mm, 30 mm, and 35 mm the maximum load obtained were 5.30 KN, 6.63 KN and 8.46 KN respectively. It is also observed that, there is an instant drops of load and move in constant manner.

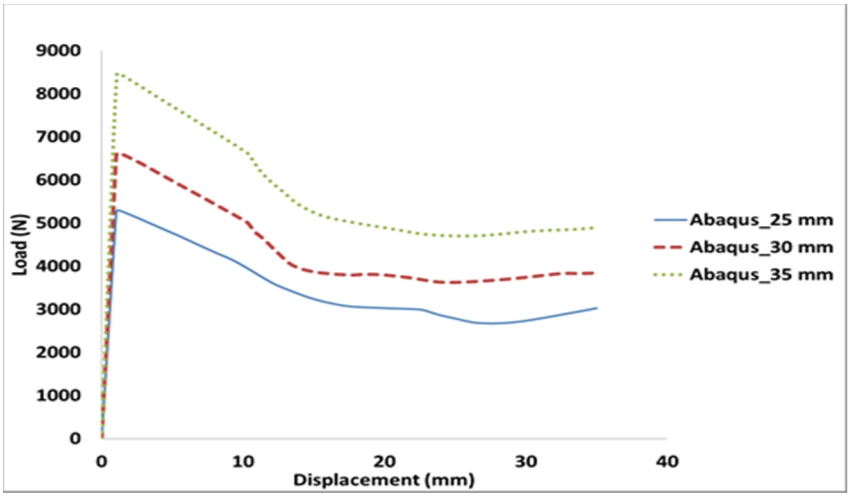

Figure 5.8 Load – Displacement curves for glass epoxy with different diameters.

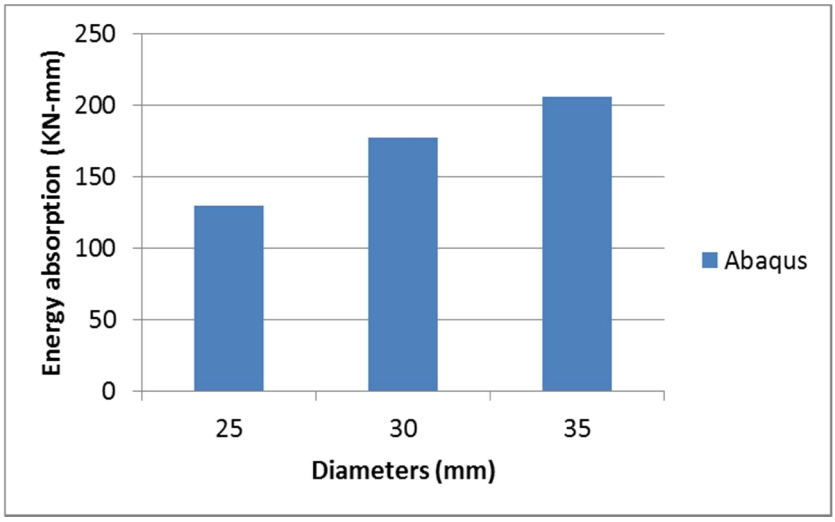

Figure 5.9 Comparison of FE simulated energy absorption capability of glass epoxy with different diameters

5.4. Comparison of experimentally obtained and FE simulated results

Figure 5.10 (a) – (e) shows graph of load - displacement curves for experimental and numerical glass/epoxy and carbon/epoxy for 1 layer, 2 layer and 3 layer composite tubes with orientation angle of 45°. The behavior of Load – Displacement graphs for the numerical composite tubes relates well with experimental results. Comparison of results showed that FE models successfully simulated the linear behavior and maximum load of the composite tubes, However Hashin failure model could not exactly predicted the behavior of composite tubes after the initial damage. The stress interactions proposed by Hashin do not always fit the experimental results, particularly in the case of matrix or fiber compression. It is well known that the moderate transverse compression ($\sigma_{22} < 0$) increase the apparent shear strength which is not predicted by Hashin's criterion. It is clearly seen that, from the visual comparison, the maximum load value obtained for both experimental and Abaqus, there is a good agreement in the results throughout the loading process. For both experimental and Abaqus, the linear portion up to the point where maximum load is reached is very close. It is also observe that, after the maximum loading

step, the experimental and Abaqus load displacement curves drop off sharply at nearly the same maximum load.

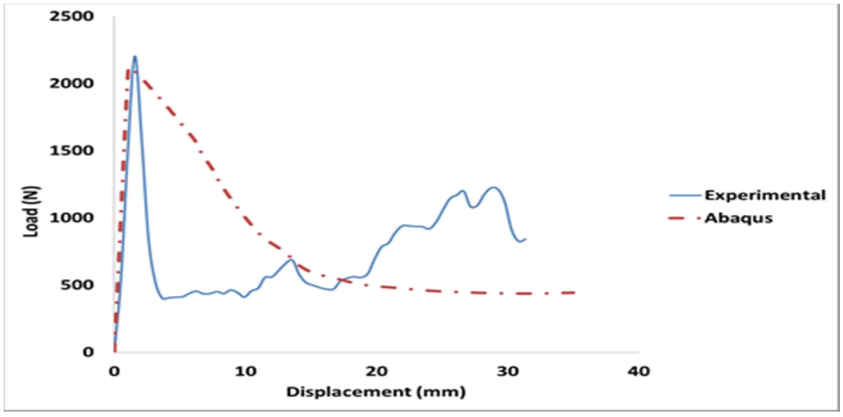

(a) Comparing experimental and FEA for 1 Layer glass/epoxy

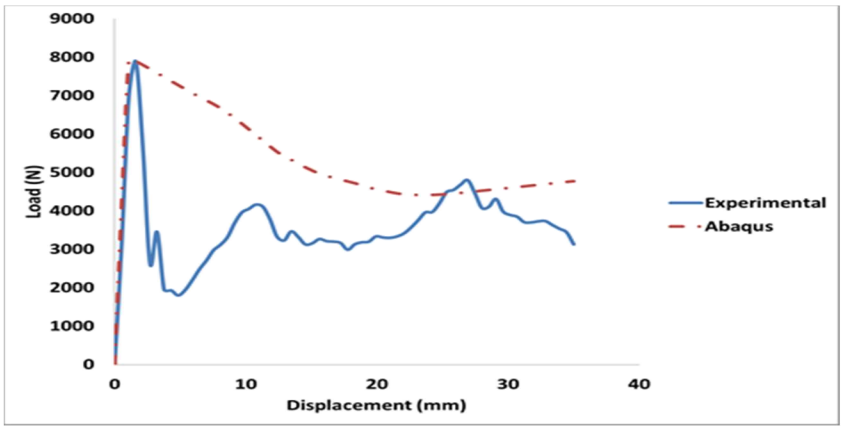

(a) Comparing experimental and FEA for 2 Layer glass/epoxy

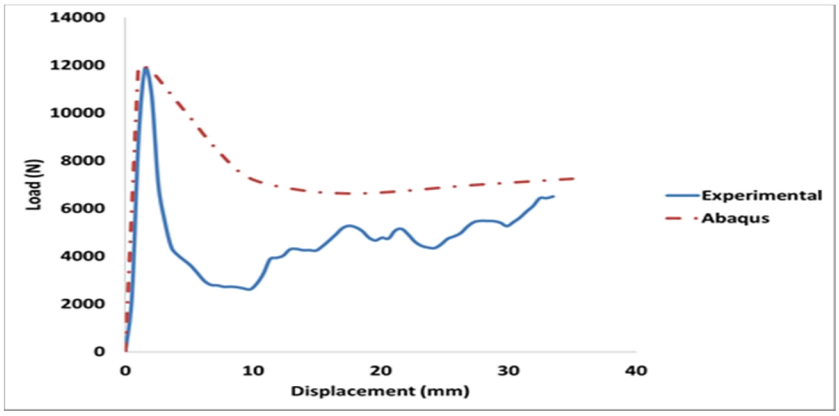

(b) Comparing experimental and FEA for 3 Layer glass/epoxy

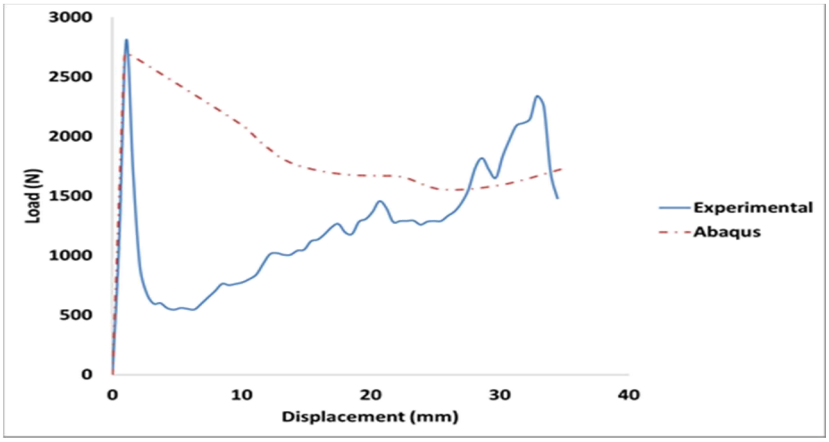

(c) Comparing experimental and FEA for 1 Layer carbon/epoxy

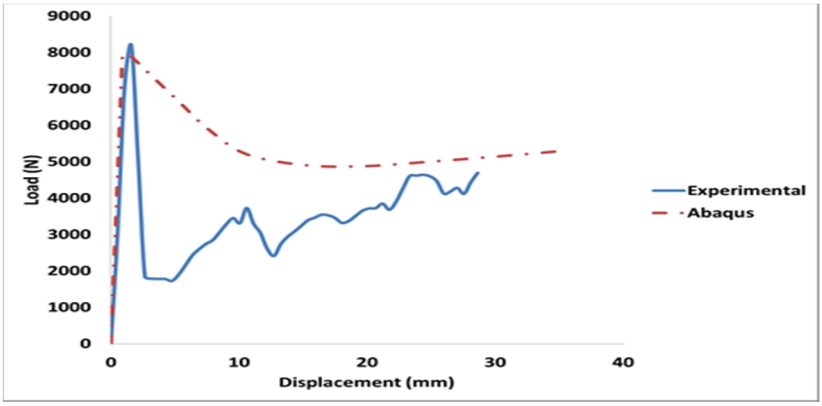

(d) Comparing experimental and FEA for 2 Layer carbon/epoxy

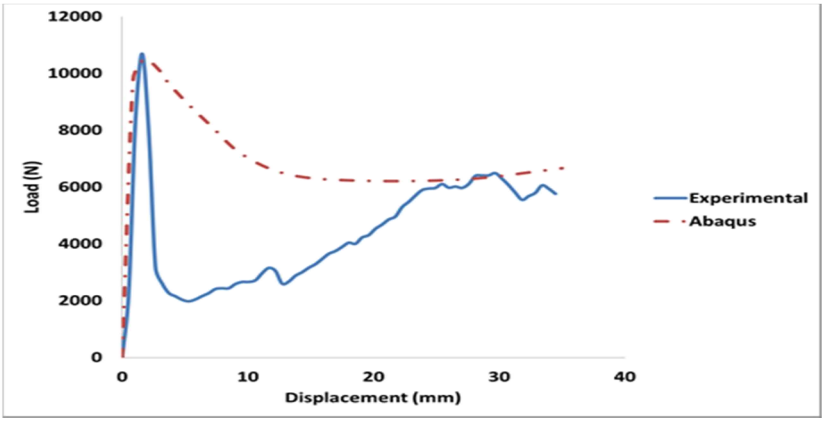

(e) Comparing experimental and FEA for 3 Layer carbon/epoxy

Figure 5.10 Comparison of experimetally obtained and FE simulated Load – Displacement relations curves of Glass/epoxy and carbon/epoxy composite tubes with different thickness

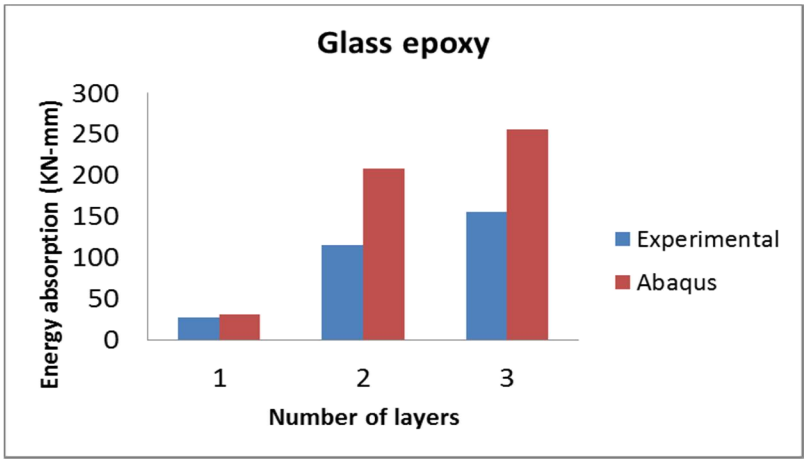

Figure 5.11 Comparing energy absorption for experimental and FEA results for glass/epoxy

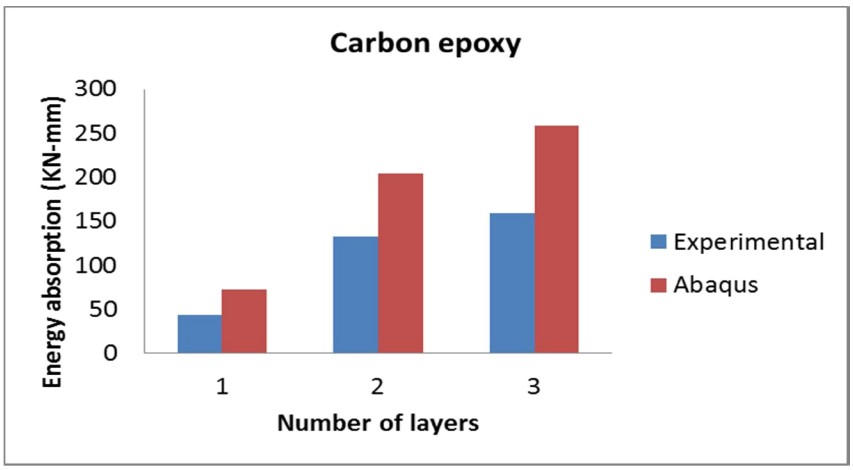

Figure 5.12 Comparison of energy absorption between simulation and experiment for carbon/epoxy with different number of layers.

Similarly, in the case of glass/epoxy with different diameters, it is clearly observed that in both experimental and numerical, load – displacement curves behaves linearly first, a considerable drop in load after reaching the maximum load is observed as shown in figure 5.13 (a) – (c). It was also seen that results obtained from finite element analysis using abaqus demonstrated constant progressive up to failure. Comparison of results showed that

FE models successfully simulated the linear behavior and maximum load of the composite tubes, However Hashin failure model could not exactly predicted the behavior of composite tubes after the initial damage. It was clearly observed from the visual comparison, the maximum load value obtained for both experimental and Abaqus, showed good agreement in the results throughout the loading process. It was also observe that, after the maximum loading step, the experimental and Abaqus load displacement curves drop off sharply at nearly the same maximum load.

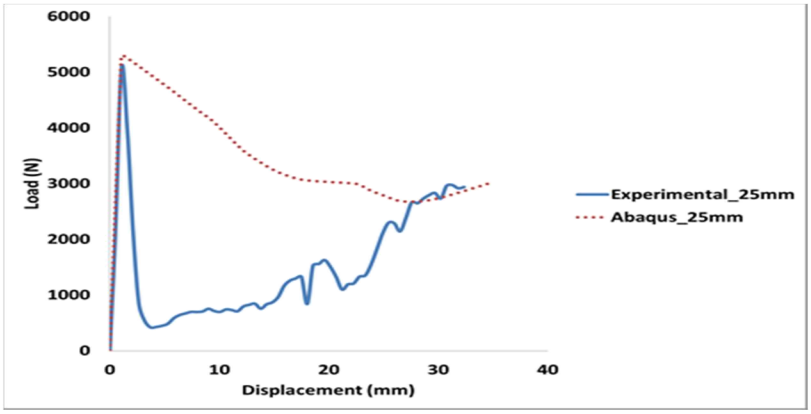

(a) Comparing experimental and FEA for 25 mm diameter glass/epoxy

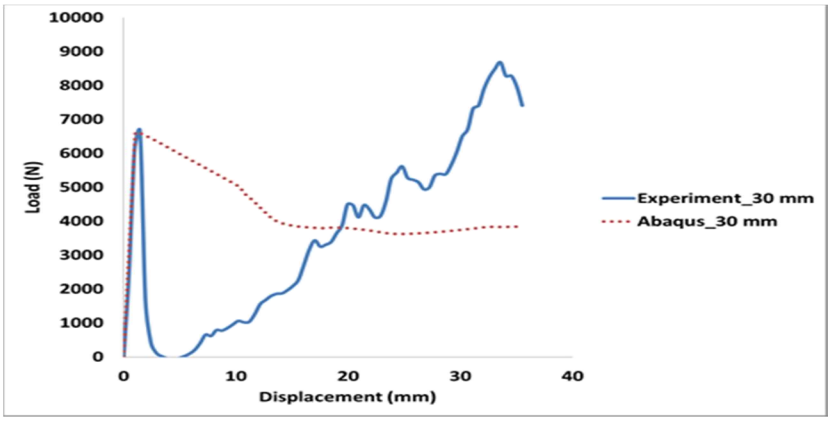

(b) Comparing experimental and FEA for 30 mm diameter glass/epoxy

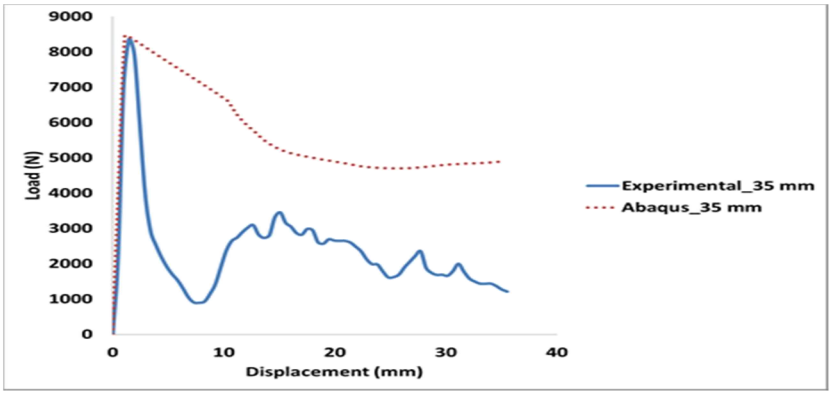

(c) Comparing experiment and FEA for 35 mm diameter glass/epoxy

Figure 5.13 (a) – (c) Load Displacement curves for comparing FEA and experimental results for glass/epoxy composite tubes with different diameters.

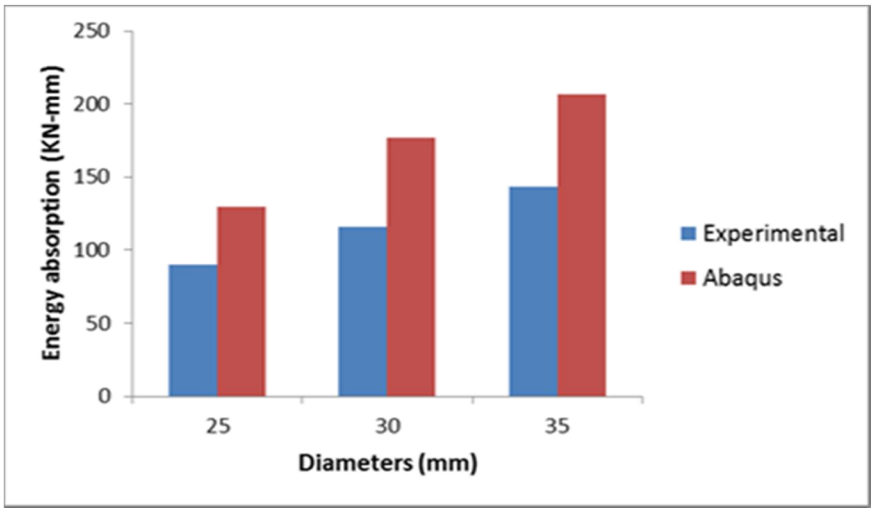

Figure 5.14 Comparison of energy absorption between simulation and experiment for glass/epoxy with different diameters.

The energy absorption for the simulation of cylindrical composite tubes was compared with experimental results as shown in Figure 5.14. In all cases similar trends have been found in terms of the maximum load and initial slope.

The reliability of finite element analysis via Abaqus has been justified against the results obtained from static compression tests of glass and carbon epoxies with varying thickness.

It has been found that the results obtained through progressive failure analysis agree reasonably well with the experimental results in the linear portion.

CHAPTER 6

CONCLUSIONS

Composite tubes were manufactured by process of filament winding. Glass and carbon fibers were selected as the reinforcement materials while epoxy resin and hardener have been used to form the matrix required for the fabrication of composite tubes. Twelve composite tubes were fabricated. Static compression test and energy absorption behavior of glass/epoxy and carbon/epoxy composite tubes were studied. During compression test, composite tubes experienced sudden breakdown mechanisms, which lead to progressive fluctuation within the vicinity of load displacement curves. Load-displacement curves deduced from this study show the same result when compared to other investigation from the literature. The parameters were studied include wall thickness, diameters and winding angles. Their effects on energy absorption were obtained, the specimen with thick layer absorb much energy absorption, the larger the diameter of the specimen the greater the energy absorption and lastly angle 35° stands much energy absorption than the others, this is due to the higher value of average crushing load and less compressive strength. Results obtained from the study shows that carbon epoxy tube stands higher load than glass epoxy. ABAQUS is used as a numerical tools using progressive damage methodology based on Hashin failure to compared the results with experimental. The Load – Displacement behavior of the simulated composite tubes correlates reasonably well with experimental results. It is interesting to note that all the experimental results behave in a similar way with simulated composite tubes where, their linear portion is almost similar up to maximum loads. Of all simulated results, Hashin failure does not give reasonable fact on brittle failure type obtained from the experiment. Also it is observed that the maximum load values obtained from the experiment correspond to the results obtained from the simulation. This validates the capability of Hashin's progressive failure in simulating damage with material linearity for composite tube with reasonable accuracy.

REFERENCES

[1] V. K. S. Choo, Fundamentals of Composite Materials, New Mexico: Knowen Academic Press, Inc.,, 1990.

[2] Ru-min Wang, et.al, Polymer Matrix Composites and Technology, Woodhead Publishing Limited, 2011.

[3] Pinar Karbuz, "Mechanical characterization of filament wound composite tubes by internal pressure testing," Masters thesis, Middle East Technical University, Ankara, 2005.

[4] N. Chawla and Krishan K. Chawla, Metal matrix composites, New York: Springer science, 2006.

[5] Autar K. Kaw, Mechanics of composite materials, New York: Taylor and Francis group, 2006.

[6] Serope Kalpakjian, Manufacturing engineering and technology, Pearson, 2009.

[7] Daniel Gay, et.al, Composite materials design and application, Wshington, DC: CRC Press, 2003.

[8] "Ceramic Fiber.Net," Mineral Seal cooperation, 2008. [Online]. Available: http://www.ceramicfiber.net/. [Accessed 18/5/2014 May 2014].

[9] P. K. Mallik, Fiber rinforced composite Materials, manufacturing and design, Dearborn, Michigan: CRC Press, 2008.

[10] F. C. Campbell, Structural composite materials, United State of America: ASM International, 2010.

[11] Sanjay K. Mazumdar, Composite manufacturing, materials, product, and process engineering, Washington, DC: CRC Press, 2002.

[12] "netcomposites," Gurit, [Online]. Available: http://www.netcomposites.com/guide/filament-winding/54. [Accessed Saturday 24 May 2014].

[13] "Wordpress," FUGAHUMANA-HUMAN FLIGHT, 12 July 2012. [Online]. Available: http://fugahumana.wordpress.com/2012/07/12/composite-manufacturing/.

[Accessed 24 May 2014].

[14] G. Lu. and T. Yu, Energy absorption of structure and materials, Washington, DC: Woodhead publishing limited, 2003.

[15] Gang Chen et.al, "7.Compressive behavior of filament wound carbon fiber/epoxy composite tube with different winding angles," *World journal of engineering,* pp. 181 - 182.

[16] Xialong Jia, et.al, "Effect of geometric factor, winding angle and pre- crack angle on quasi static crushing behaviour of filament wound CFRP cylinder," *Composite: part B,* vol. 45, pp. 1336 - 1343, 2013.

[17] Wieslaw Barnat, et.al, "Composite polymer materials for energy absorbing structures," *Journal of KONES Powertrain and transport,* vol. 16, 2009.

[18] S. H. Lee and Anthony M. Waas, "Compressive response and failure of fiber reinforced unidirectional composites," *International Journal of fracture,* vol. 100, pp. 275 - 306, 1999.

[19] Stanislaw Ochelski and Pawel Gotowicki, "Experimental assessment of energy absorption capability of carbon-epoxy and glass-epoxy composites," *Composite structures,* vol. 87, pp. 215 - 224, 2009.

[20] A. S. Abosbaia, et.al, "Energy absorption capability of laterally loaded segemented composite tubes," *Composite structures,* vol. 70, pp. 356 - 373, 2005.

[21] Farley G. L., "Energy absorption of composite materials," *Journal of composite materials,* vol. 17, pp. 267 - 279, 1983.

[22] Gary L. Farley, "Relationship between mechanical properties and energy absorption trends for composite tubes," National aeronatics and Space administration, Washigton, DC, 1992.

[23] Hong- Wei Song, et.al, "Axial impact behaviour and energy absorption efficiency of composite wrapped metal tubes," *Int. J. of Impact Engineering,* vol. 24, pp. 385 - 401, 2000.

[24] George C. Jacob, et.al, "Energy absorption in polymer composites for automotive crashworthiness," *Journal of composite materials,* vol. 36, pp. 813 - 838, 2002.

[25] Sivakumar Palanivelu, et.al, "Crushing and energy absorption performance of different geometrical shapes of small scale glass/polyester composite tubes under quasi static loading conditions," *Composite structures,* vol. 93, pp. 992 - 1007, 2011.

[26] Jose Daniel D. Melo, et.al, "The effect of processing conditions on the energy absorption capability of composite tubes," *Composite structure,* vol. 82, pp. 622 -

628, 2008.

[27] Libo Yan, et.al, "Effect of triggering and polyurethane foam filler on axial crushing of natural flax/epoxy composite tubes," *Materials and Design,* vol. 56, pp. 528 - 541, 2014.

[28] Ping Zhang, et.al, "Finite element modeling of the quasi- static axial crushing of braided composite tubes," *Computational Materials Science,* vol. 73, pp. 146 - 153, 2013.

[29] F. Mustapha and N. W. Sim, "Investigation of axial crushing behavior of a composite fuselage model using the cohesive elements," *Journal of theoritical and applied mechanics,* vol. 50, no. 2, pp. 531 - 548, 2012.

[30] Rizal Zahari,et.al, "Prediction of progressive failure in woven glass/epoxy composite laminated panels," *Jurnal Mekanical,* vol. 25, pp. 80 - 91, 2008.

[31] Flexwind, Advanced filament winding control, Mcclean Anderson, 2007.

[32] Hexion Technical Information, Epoxy and phenolic resin division, Germany: Stuttgart, 2006.

[33] "Cam Elyaf Sanayii A.Ş," Camelyap glass fiber, 2009. [Online]. Available: http://www.camelyaf.com/products/detay.aspx?SectionID=KQ7P%2fvTrYtZ3H72wsLTnJw%3d%3d&ContentID=MUGCVXsj6bt%2fDFgPjI9PdQ%3d%3d. [Accessed 24 May 2014].

[34] Dowaksa, "Technical data sheet," Aksaca, Istanbul, 2012.

[35] N. H. Yang, et.al, "Multi-axial failure models for fiber reinforced composites," *Journal of ASTM International,* vol. 4, no. 2, 2007.

[36] Ercan Sevkat and Hikmet Tumer, "Residual torsional properties of composite shafts subjected to impact loadings," *Materials and Design,* vol. 51, pp. 956 - 967, 2013.

[37] ABAQUS User's Manual, Volume 1 - 3, 2003.

[38] Joy Pederson, "Finite element analysis of carbon composite ripping using Abaqus," Masters thesis, Clesmon University,, 2006.

[39] Vladimir Sokolinsky, "Using failure criteria for unidirectional fiber composites in Abaqus," Simulia, 2013.